# A FEASIBILITY STUDY ON USING SURFACE TREATED KAOLIN MINERAL IN THERMOPLASTIC COMPOSITES

A Dissertation
Presented to
The Academic Faculty

by

Mohamed Gamal Shafik Baioumy

In Partial Fulfillment
of the Requirements for the Degree
Master's of Science in the
George W. Woodruff School of Mechanical Engineering

Georgia Institute of Technology
May 2017

# A FEASIBILITY STUDY ON USING ULTRAFINE SURFACE TREATED KAOLIN MINERAL IN THERMOPLASTIC COMPOSITES

Approved by:

Dr. Kyriaki Kalaitzidou, Advisor
School of Mechanical Engineering
*Georgia Institute of Technology*

Dr. Jonathan Colton
School of Mechanical Engineering
*Georgia Institute of Technology*

Dr. John Poulakis
IMERYS Minerals

Date Approved:  April 24th, 2017

Dedicated to my family for I could not and would have not reached this point without their support.

# ACKNOWLEDGMENTS

# TABLE OF CONTENTS

# LIST OF TABLES

# LIST OF FIGURES

# LIST OF SYMBOLS AND ABBREVIATIONS

EPA    Environmental Protection Agency

CFRP    Carbon Fiber Reinforced Plastic

mIM    Micro Injection Molding

MIM    Macro Injection Molding

NP    Nylon Pellet

GF    Glass Fiber

% ML    Percent Mass Loss

TGA    Thermogravimetric Analysis

MRF    Modulus Reduction Factor

HDT    Heat Deflection Temperature

SEM    Scanning Electron Microscopy

MRF    Modulus Reduction Factor

# SUMMARY

Glass fiber reinforced plastics are the current state of the art, mainly in automotive manufacturing applications. With the industry's trend towards weight reduction for fuel economy and enhanced performance, an improvement in material composition is needed. This thesis investigates the possibility of using surface-treated kaolin mineral fillers as a substitute or a complement to glass fibers in nylon composites. An experimental approach is utilized to determine their properties and compare them to existing materials in the industry. Specimens are fabricated using a twin-screw tabletop micro-extruder for the first phase of the study, and a 75-ton injection molding machine, which compares to the industrial standard, for the second phase. Mechanical tests, thermal tests, and density measurements are used to evaluate the composite material properties. SEM imaging is used to investigate filler morphology and its distribution within the matrix, as well as voids and defects. A comparison between lab-scale and scale-up fabrication techniques is used to highlight the effects of manufacturing conditions. A micromechanical model is employed to compare experimental results to theoretical predictions. Results suggest that high aspect ratio fillers increase the strength and stiffness of the composite. Conversely, low aspect ratio particles improve impact strength. Furthermore, particle size affects the dispersion of the mineral, with minerals predicted to have a smaller particle size showing less agglomeration. Blending multiple mineral morphologies showed a synergistic effect in resulting properties. Similar trends were found in both phases of the study indicating that lab scale fabrication can be used as a screening to investigate the reinforcing ability of the minerals.

# CHAPTER 1.    INTRODUCTION

## 1.1    Background

The effects of fuel economy have recently become of significant importance in automotive body part design. An unstable oil industry and increasing environmental awareness have left auto designers staggering to make their vehicles more fuel-efficient. In addition to that, recent legislation has been pushing auto manufacturers into making lighter weight cars. By 2025, the U.S. Environmental Protection Agency (EPA) requires the market average fuel economy for American made cars to be 54.5 mpg, up from 34.5 in 2016 [EPA 2016]. This has put automakers on a strict schedule. Decreasing the overall weight of vehicles is one of the methods car designers use to increase fuel efficiency. EPA standards estimate that a 100-lb. reduction in vehicle weight improves fuel economy by 1-2% [EPA 2016]. In addition, every kilogram reduction in car weight can correspond to a 20-kg reduction in greenhouse gas emissions throughout the lifetime of a vehicle [Fisher et al.].

Previous efforts in vehicle weight reduction are mainly characterized by three phases in automotive development. These are architectural, motor efficiency, and alternative material based. In the mid 1970's, the average weight of road vehicles peaked. This can be seen in Figure 1, which shows the progression of the weight of passenger cars in the US since 1975. This increase was mainly motivated by safety and performance concerns rather than fuel efficiency. In the early 1980's, however, significant strides in the development of unibody car frames caused an average drop of 450 kgs (1000 lbs.) in vehicle curb weight over the span of four years [Mackenzie et al. 2012]. This design that

employed a unified chassis and body structure instead of a body on frame structure allowed for smoother stress transfer, which decreased the amount of material needed to maintain frame sturdiness. The development of front-wheel drive cars reduced the amount of drive train components and contributed to the general weight reduction of the vehicle. Advances in engine technology have also allowed carmakers to extract more power out of a given engine mass. The increasing popularity of paired configuration engine cylinders e.g., (4,6,8 cylinders) has made engines leaner as opposed to odd numbered (3 and 5) cylinder engines [Mackenzie et al. 2012].



**Figure 1 - Average curb weight of US cars and trucks [Mackenzie et al 2012]**

**Table 1 - Relative weight savings of some alternative materials**

| Material | Weight Savings Potential (%) |
|---|---|
| Conventional Steel | 0% |
| Iron | 0% |
| High-Strength Steel | 23% |
| Aluminum | 45% |
| Magnesium | 60% |
| Plastics and Composites | 50% |

However, after the sharp decline in the 1980's, vehicle weight started to stagnate and even increase slightly due to growing performance requirements. As other weight reducing methods started to saturate, designers began considering alternative materials as a possible solution to reducing vehicle weight. Traditional materials, like low-carbon steel and iron, now make up less than half the weight of new vehicles [Mackenzie et al 2012]. Alternative materials, like light weight metals (aluminum and magnesium) and plastic composites, have been recognized as weight savers for automotive structures. Table 1 above shows the weight saving potential for some alternative automotive materials. It can be noted that substituting steel for composite plastic materials can result in a 50% weight reduction. For this reason, composites are currently on the hot plate for automotive manufacturers. The

following sections discuss different types of composites used in the automotive industry, as well as past and future efforts for the integration of composites in car design.



With continuous fiber-reinforced thermoplastic composite parts, the best possible combination of weight savings, cost efficiency and performance can be achieved for body and chassis.

Structural support for door module

Roof crossbeams

Bumper stiffener at rear

Structural rear tray

Structural inner shell for trunklid/tailgate

Dashboard crossbeam

Structural inner shell for hood

A, B, C pillar reinforcement

Structural battery casings

Seat structures

Structural floor module

Bumper stiffener at front

Structural front end

Firewall

**Figure 2 - Distribution of common composite structures in cars [BASF 2017]**

## 1.2    Composites in Automotive

An increase in the use of composites for automotive applications has been seen in recent years. It is estimated that 50% of a car volume (10% wt.) on average is now made of composites and plastics [Fisher et al.]. Moreover, some recent models have bodies made entirely from reinforced plastics. Figure 2 shows a distribution of body parts where composites are a popular choice. With a wide range of properties required for each

application, e.g. impact strength is important for the bumper while thermal characteristics are more relevant for a composite firewall, different types of composites are being used.

### 1.2.1 Fiber Reinforced Plastics

Fiber reinforced plastics are characterized by thermoplastic or thermoset matrix materials with fibers added to improve properties. When combined, composite constituents perform better than they would separately. Carbon fiber, glass fiber, and Kevlar are popular reinforcement options, while epoxy and nylon are common matrix materials. Carbon-fiber composites weigh about one-fifth compared to steel, but are as good or better in terms of stiffness and strength. Also, they also do not rust or corrode like steel, aluminum, or magnesium. They could significantly increase vehicle fuel economy by reducing vehicle weight by as much as 60 percent [Das 2001]. Due to this high strength to weight ratio, they are often used for structural applications and vehicle frames. The BMW i3, for instance, utilizes a body on frame structure made entirely from carbon fiber reinforced plastic (CFRP) [BMW 2017].

However, carbon fibers incur a high material cost [Das 2017], which limits their potential usage. They are usually more complex to process and, as they used mainly with thermosets, the production rate could be limited due to the required curing time. Glass fibers, on the other hand, are less stiff than carbon fibers. However, they have certain characteristics that make them more attractive than carbon fibers for certain applications. Pound for pound, carbon fibers are four to six times as expensive as glass fibers [Das 2017]. In addition, chopped strand glass fibers can be cheaply mass-produced with a thermoplastic matrix using injection molding. These factors make glass fiber composites a lucrative

option for high volume automotive applications. They are a popular option for battery enclosures, gas tanks, valve covers, air intake manifolds, bumpers, and, to a lesser extent, body panels [BASF 2017].

Nevertheless, there are drawbacks to fiber reinforced composites that designers are looking to overcome. First, fiber composites often have an unbalanced profile of properties. Carbon fibers for instance have impressive strength-to-weight tensile and flex properties, however, concerns about their toughness have led to speculations about their crashworthiness [Zhou et al. 2015]. Glass fibers on the other hand are more impact resistant but are less stiff [Bagherpour 2012]. Multi fiber composites have been proposed as a solution; however, issues of homogeneity and fiber-fiber interactions arise [Li et al. 1995]. Glass fibers also accelerate tool wear due to their abrasive nature. Under high injection pressures, the mechanical rubbing of glass fiber tips on mold and screw surfaces introduces scratches that result in undesirable surface characteristics in the finished product [Silva et al. 2017]. Equipment then must be maintained and replaced more often, which adds to the final processing cost, increases downtime, and decreases throughout. The dimensional stability of plastics has also been an issue that designers have been trying to improve. The anisotropic nature of fiber composites further aggravates this problem [Wolff 2004].

### 1.2.2   Fillers in Composites

Composite fillers are particles with different morphologies mixed and embedded within the matrix to improve certain characteristics. Unique property combinations are achievable with fillers. For instance, they can be used to modify density, increase stiffness and strength, improve impact resistance, hedge polymer degradation, and prevent fiber

hang-ups in dies to improve cycle time [Wiebking 1998]. Traditionally fillers were low cost large particle materials added to formulations to lower cost by simply "filling" in for more expensive counterparts. Recently, however, fillers are being treated as true performance additives. Advances in compounding methods have allowed for much finer particle size. Fillers can now be modified, tailored, and mixed to cater to a wide range of properties in composites. Mineral fillers are popular in polymer composites due to their low price, wide range of properties, and relative ease of processing. Powder fillers show potential to solve some of the challenges of fiber composites discussed in the previous section. Carbonates, kaolin, and talc are widely used as mineral fillers in thermoplastic composites.

Table 2 shows select properties of fillers and the impact they have on a composite's properties. A general characteristic used to group and rank fillers is particle size. The particles used in this thesis fall in the micron or submicron range. Particle size has a direct effect on the final properties of the composite, mainly impact strength and stiffness. Onuegbu et al. showed an inverse relationship between impact strength and filler particle size in polypropylene [Onuegbu et al. 2011]. Wiebking showed a similar relationship for carbonate fillers in PVC [Wiebking 1998].

**Table 2 - Representative filler characteristics**

| Filler Property | Range | Effect on composite |
|---|---|---|
| Particle Size | Ultrafine to Large | Impact Strength ↑ with Particle Size ↓ |
| Particle Shape | Plate like - Blocky | Plate like - $E_y$↑ $E_{flex}$↑ Blocky - Impact Strength↑ |
| Fusion & Adhesion | Weak to Very Strong | $E_y$↑ , Tensile Strength↑ with Adhesion ↑ |
| Dispersion | Poor to Very Good | Impact Strength ↑ $E_y$↑ $E_{flex}$↑ with Dispersion ↑ |

Aside from the size, fillers also come in a variety of shapes. Acicular particles, spheres, platelets, as well as irregular shapes are common. An important characteristic of shape is aspect ratio; this is the ratio of the particle's largest to smallest dimension as shown by Figure 3 below. Wiebking showed a positive relation between aspect ratio and stiffness, which is examined during the course of this study.

Strong interfacial adhesion between the constituents of a composite is required for good mechanical performance. Thus, a good filler should have a strong affinity to bond with polymer matrix and adhere to the surface of any fibers used. A mutual affinity between the polymer, fiber, and filler could increase their interfacial strength [Mallick 2008]. This

shows a profound effect on tensile properties as it allows for a more cohesive stress transfer during elongation.
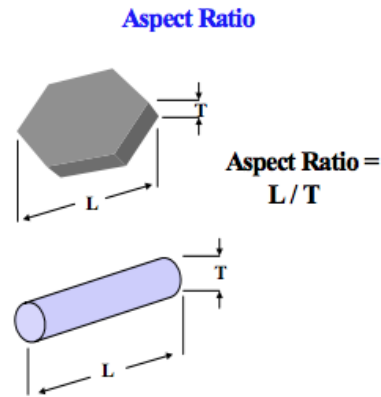


**Figure 3 - Aspect ratio of particles [Wiebking 1998]**

In addition to adhesion, fillers must be well dispersed within the matrix to achieve desirable effects. Sufficient shear needs to be applied to break any agglomerates and evenly disperse filler particles within the matrix. The manufacturing method and processing conditions have a direct effect on the dispersion achieved. Longer mixing time and higher screw RPM are viable options to increase dispersion. However, an optimum processing window exists in order to avoid thermal degradation, from mixing the polymer for too long, or shear degradation, from mixing it too hard. Twin screw compounding machines have been shown to achieve better dispersion at lower RPMs and mixing times [Raj et al 2015]. This allows finer particles to be processed while maintaining sufficient dispersion.

Surface treatment and hardness are also some characteristics worth mentioning in the scope of this study. Surface treatment can be applied to fillers to decrease agglomeration,

improve their dispersion within the matrix, and improve their affinity to bond onto fibers. Different surface treated fillers are utilized during this study. Tool wear is directly related to particle size and material hardness. Larger and coarser particles result in more abrasion to processing tools. The particles in this study are in the micron to submicron range and pose little abrasion to tools.

## 1.3    Kaolin in Thermoplastics

The filler of interest in this study is kaolin. Kaolin is a white mineral clay that naturally occurs in rock deposits. It has an inorganic structure - $Al_2Si_2O_5(OH)_4$. Kaolin is characterized by its fine particle size, plate-like lamellar structure, and chemical inertness. Kaolin has been widely used as resin extender in plastics and rubber and as a viscosity modifier in paints. Advances in processing and surface treatment techniques have allowed for improved usage as a performance enhancer. A brief overview of representative studies where kaolin has been used is given here. Guessoum et al. have shown that kaolin enhances thermal stability in polypropylene [Guessoum et al. 2012]. A study by Raj et al. suggests that kaolin can be used to enhance mechanical properties and improve scratch resistance in some commercial polymers [Raj et al. 2015]. Unal et al. experimented with non-surface-treated kaolin and talc in a nylon 6 matrix and found improvements in tensile strength and modulus but a decrease in ductility and impact strength [Unal et al. 2003].

## 1.4    Problem Statement and Motivation

The effects of fuel economy have recently become of significant importance in automotive body part design. An unstable oil industry and increasing environmental awareness have left auto designers staggering to make their vehicle designs more efficient.

Substituting lightweight materials in place of traditional heavy metals has been one of the methods designers use to improve vehicle design. Of particular importance to this study are glass fiber composites, commonly used for their light weight and diverse properties. However, glass fibers are associated with certain drawbacks and have an abrasive nature. Kaolin fillers have shown good potential as performance additives in thermoplastic materials. The addition of kaolin filler to automotive composite materials can improve some of the characteristics of glass fiber composites for manufacturers. This thesis investigates the possibility of using surface-treated kaolin mineral fillers with varying morphologies to replace or extend glass fibers in nylon composites. An experimental approach will be utilized in which different reinforcement-filler formulations will be examined and their properties thoroughly assessed. The challenges and benefits of using each these materials (glass fiber vs glass fiber and mineral) will be addressed and a comparison between different compositions and fabrication conditions will be highlighted.

## 1.5    Goals and Objectives

The goal of this research is to investigate the effects of introducing kaolin fillers in nylon-glass fiber composites. This will be achieved through three objectives. First, composite specimens will be fabricated using lab scale micro extrusion and injection molding units. This will include an assessment of the performance of different kaolin mineral fillers in unreinforced nylon and glass fiber reinforced nylon. Sets of composites will be fabricated using a common weight percentage (30% wt.) of kaolin fillers with varying properties (surface treatment, particle size and shape). Composites with 25% wt. mineral and 5% wt. glass fiber will also be made. The properties are to be compared against 100% unfilled nylon and 30% glass fiber loading composite. One set of mineral composites

will be fabricated at 40% mineral loading to investigate the effects of varying mineral composition. A hybrid batch, made with a blend of two kaolin minerals, will be fabricated to investigate the synergistic interactions between kaolin fillers.

The second objective of this research is to determine whether or not the effect of the minerals on the properties of the polymer or/and of the glass fiber/polymer composites shows the same trend when the composites are made using large scale injection molding unit. The properties of composites made using equal fiber to mineral ratios will be determined. Batches of pure nylon and glass fiber only composites will be benchmarked as controls.

The third objective is to utilize a micromechanical model, namely the Halpin-Tsai model, in order to determine the reinforcing efficiency of the minerals by comparing the theoretical predictions with the experimentally determined modulus. A parametric study is also performed to obtain a rough estimate of the modulus of kaolin as this property is not available by the minerals' manufacturer.

Therefore, tasks performed to realize the objective of the study are:

1) Investigate the effects of kaolin addition on the properties of nylon composites using microscale fabrication. This will be accomplished by the following:
    - Fabricate composites containing mineral only and mineral-glass fiber and compare their mechanical and thermo-mechanical properties.
    - Fabricate composites containing two types of kaolin minerals to investigate possible synergistic effects.
    - Determine the properties of composites, for a given mineral as a function of the mineral loading up to 40 wt%.
    - Study fiber-filler interactions within the composite and compare all batches.

2) Investigate the effects of process parameters on the composites properties by comparing the properties of composites made using lab-scale and large scale injection molding.

3)  Determine the reinforcing efficiency of the minerals by comparing theoretical predictions of modulus obtained using the Halpin-Tsai model to the experimentally determined moduli.

## 1.6    Thesis Organization

This thesis consists of five chapters:

Chapter (1): A brief introduction about the topic, a discussion of different types of composites, and a review of kaolin minerals and properties of mineral filled composite materials are presented. This chapter introduces the problem statement and the objectives of the research.

Chapter (2): The research methodology and the experimental procedure are discussed. The materials used and the techniques employed to fabricate and characterize the composites are presented in detail.

Chapter (3): The experimental results obtained from the first objective of this study are presented and discussed.

Chapter (4): The experimental results obtained from the second objective of this study are presented and discussed.

Chapter (5): A comparison between theoretical predictions experimental results in terms of the tensile modulus is provided.

Chapter (6): A summary of the study, including its main conclusions and recommendations for future work, is provided.

# CHAPTER 2.    MATERIALS AND METHODS

## 2.1    Materials

The polymer of interest in this study is nylon-6. This choice was made based on its desirable thermal and mechanical properties and its prevalence of the material in automotive applications [BASF 2001].  Since understanding the bonding interactions of kaolin in the polymer matrix is important, it was decided to conduct a direct study on nylon composites instead of a comparative study on kaolin minerals in a generic matrix common across test batches. The choice of nylon, however, presented a set of processing challenges.

First, nylon-6 is a highly hygroscopic resin. Previous studies have shown water saturation of up to 2.5% wt. at room conditions and 10% wt. when submerged in water for 1 week at 40 $^\circ$C [DuPont 2001]. To overcome this, the nylon was dried pre-processing and double bagged in vacuum-sealed polyethylene bags. Different drying conditions were explored and are discussed in section 2.2. To ensure dryness, the nylon was taken out of the bag and dried a second time immediately before processing.

Second, nylon-6 has a relatively narrow processing window compared to other polymers. The onset of thermal degradation starts 30°C above its melting point and small changes in the injection cycle can cause a defective part [DuPont 2001]. This required a close monitoring of temperature and pressure settings during processing. TGA (Thermogravemetric Analysis) was also employed to monitor the moisture content and degradation of samples before and after processing. The nylon used was of grade B-27E acquired from BASF.

Ten-micron glass fiber rovings of grade ME1510 acquired from Owens Corning were used as reinforcement. The rovings were chopped in house to 1/4" ± 1/8" for processing. Being proprietary in nature, little information is available about the sizing applied to the fibers. However, it is predicted to be silane in nature [Owens Corning 2014].

Kaolin fillers were provided by IMERYS and were used as received in this study. The fillers were classified by mineral content and surface treatment applied. The fillers were given generic names as the information for their exact compositions is proprietary. The filler names are given in the form XP15-0XY1-Z where X represents a different family of particle morphology and Y and Z represent different processing conditions and surface treatments. In addition to these minerals, a similar commercially available product from BASF, namely Translink 445, was used for comparative purposes.

## 2.2 Fabrication Techniques

As nylon is a hygroscopic material, the first step was to dry the nylon (or composite) pellets to eliminate any trapped moisture. A 2000 W vacuum oven with a 30 inHg suction pump was used. The drying temperature was set to 80°C and the pellets were left to dry for 3±0.25 hours. The nylon was then immediately transferred to double polyethylene vacuum bags and stored till needed. Samples were taken from the bags at irregular time intervals to monitor their moisture level using TGA. Immediately before processing the nylon and the mineral filler were dried for three more hours at 80°C. The two-stage drying was done to prevent thermal degradation or discoloration from prolonged drying in one step [DuPont 2001]. During large-scale fabrication, bubbles were observed in some of the injection

molded composite specimens. Consequently, the temperature during second stage of drying was increased to 100°C to ensure sufficient dryness.

In order to investigate the performance of kaolin fillers, multiple sets of composites with different glass fiber content and reinforcement and filler content and type were fabricated. Melt compounding followed by injection molding was the processing method of interest using either lab-scale or large-scale equipment. In the first method, the samples were fabricated using tabletop micro extruder connected with a transfer mold with a micro injection-molding unit. These are shown in Figure 4.
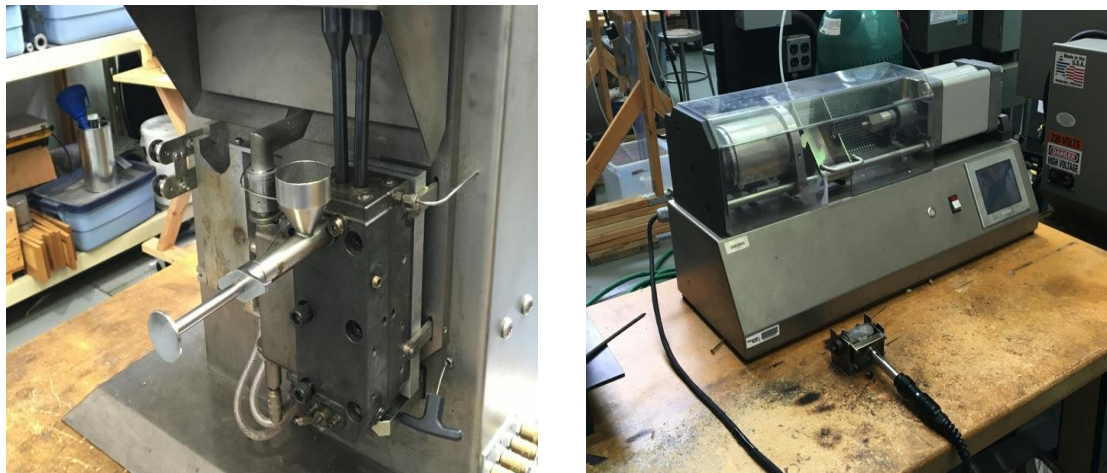


**Figure 4 - Micro extrusion (left) & injection molding unit with transfer gun (right)**

Ten grams of total material were weighed out in small cups according to the composition needed. No premixing was applied. The material was then fed into the extrusion barrel through the hopper with the coarser polymer pellets being introduced in the hopper last to prevent the finer mineral particles from accumulating at the top of the barrel. The material was then left to mix in the barrel for 3 minutes. The RPM of the screws was set to 100. The temperatures on the extruder and molding unit are shown in Table 3.

Post compounding, the melted material was transferred to the micro injection-molding machine using the transfer gun and molded to the required shape.

**Table 3 - Temperatures in extruder, transfer gun and mold**

| Barrel | Melt | Transfer gun | Mold |
|--------|------|--------------|------|
| 250°C | 230°C | 240°C | 80°C |

Flex coupons with dimensions of 63.5x12.8x3.2 mm and dog-bone specimens sized based on ASTM D638 type V bars [ASTM 2017], both shown in Figure 5, were made. The injection cycle was set to 8 bar for 5 seconds followed by 12 bar for 10 seconds. The formulations made are shown in Table 4.
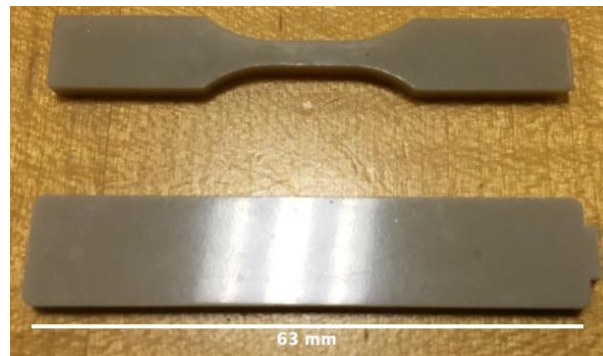


**Figure 5 - Coupons molded using table top extruder. Type V tensile bar (top), Flex bar (bottom)**

**Table 4 - Formulations made using micro injection molding**

| Batch ID | Filler 1: (wt. %) | Filler 2: (wt. %) | Nylon (wt. %) | GF (wt. %) |
|---|---|---|---|---|
| mIM-Nylon | - | - | 100% | - |
| mIM-1 | XP15-0621: 30% | - | 70% | - |
| mIM-2 | XP15-0721: 30% | - | 70% | - |
| mIM-3 | XP15-0831: 30% | - | 70% | - |
| mIM-4 | XP15-0641: 30% | - | 70% | - |
| mIM-5 | XP15-0641: 40% | - | 60% | - |
| mIM-6 | XP15-0621: 15% | XP15-0831: 15% | 70% | - |
| mIM-7 | XP15-0621: 25% | - | 70% | 5% |
| mIM-8 | XP15-0721: 25% | - | 70% | 5% |
| mIM-9 | XP15-0831: 25% | - | 70% | 5% |
| mIM-10 | XP15-0641: 25% | - | 70% | 5% |
| mIM-11 | Translink 445: 25% | - | 70% | 5% |
| mIM-12 | - | - | 70% | 30% |

The second phase of fabrication utilized large scale manufacturing techniques. The setup used is shown in Figure 6. Dog-bone and flex bar samples made for this phase are shown in Figure 7. The dimensions for flex bars were 128 x 12.8 x 32 mm. The flex bars were cut in half using a band saw before testing to fit the testing frame. Tensile coupons were sized in accordance to ASTM D638 type I bars [ASTM 2017].



**Figure 6 - Industrial sized injection molding machine**
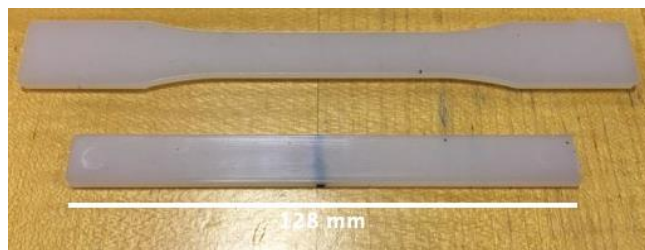


**Figure 7 - Injection molding dog-bone (top) and flex bar (bottom) samples marked halfway**

It was initially planned to utilize a one-step compounding and molding process in an industrial sized 75-ton single-screw injection-molding machine. However, the machine available in house had areas of narrow screw flight and a non-compounding nozzle system that ran the risk of being jammed with raw glass fiber. In addition, twin-screw machines were shown to achieve better mixing over single screw machines [Raj et al 2015]. Therefore, the compounding was done in batches on the small twin-screw top-bench micro extruder. The conditions used were slightly different than the conditions used during the first phase of the study, i.e., lab-scale fabrication of composites. Specifically, the RPM was increased to 150 and the mixing time was dropped to 2 minutes to account for further mixing during the injection molding step. Instead of collecting the material in the transfer gun, continuous strands were collected and pelletized to an average length of 1/4". The composite pellets were then dried and used to fabricate composite testing coupons on the large-scale injection molding unit.

The first attempt resulted in testing coupons with entrapped bubbles. It was suspected to be due air/moisture bubbles or shrinkage voids. A desiccator hopper was mounted on the machine to ensure the pellets do not absorb moisture while waiting to be fed into the barrel of the injection molding unit. With the pellets being dried before processing and fed from a dry hopper, moisture entrapment became unlikely. The issue, however, did not resolve.

It was hypothesized that increasing the packing pressure could eliminate the bubbles by forcing more material into the mold to fill any voids. The pressure was progressively increased until the onset of flashing. This, however, caused more bubbles to appear. This increase could potentially be attributed the high pressure forcing the mold

cavity open relieving pressure on the part and disturbing the packing pressure. Based on literature recommended packing pressure values, the injection pressure was decreased to two-thirds of the maximum injection pressure [DuPont 2001]. This eliminated the bubbles from the produced parts. A demonstration of the progression of sample quality is shown in Figure 8. The processing conditions are shown in Table 5 and Table 6. The formulations made are shown in Table 7.

**Table 5 - Process parameters for macro injection molding**

| Hold time | Shot size | Screw RPM | Clamp force | Hold pressure |
|-----------|-----------|-----------|-------------|---------------|
| 20 sec | 45 mm | 60 | 75 tons | 1.8 MPa |

**Table 6 - Temperatures in macro injection molding machine zones**

| | Melt | Zone 6 | Zone 5 | Zone 4 | Zone 3 | Zone 2 | Zone 1 |
|--|------|--------|--------|--------|--------|--------|--------|
| Set temperature | 235°C | 240°C | 240°C | 235°C | - | 230°C | 225°C |
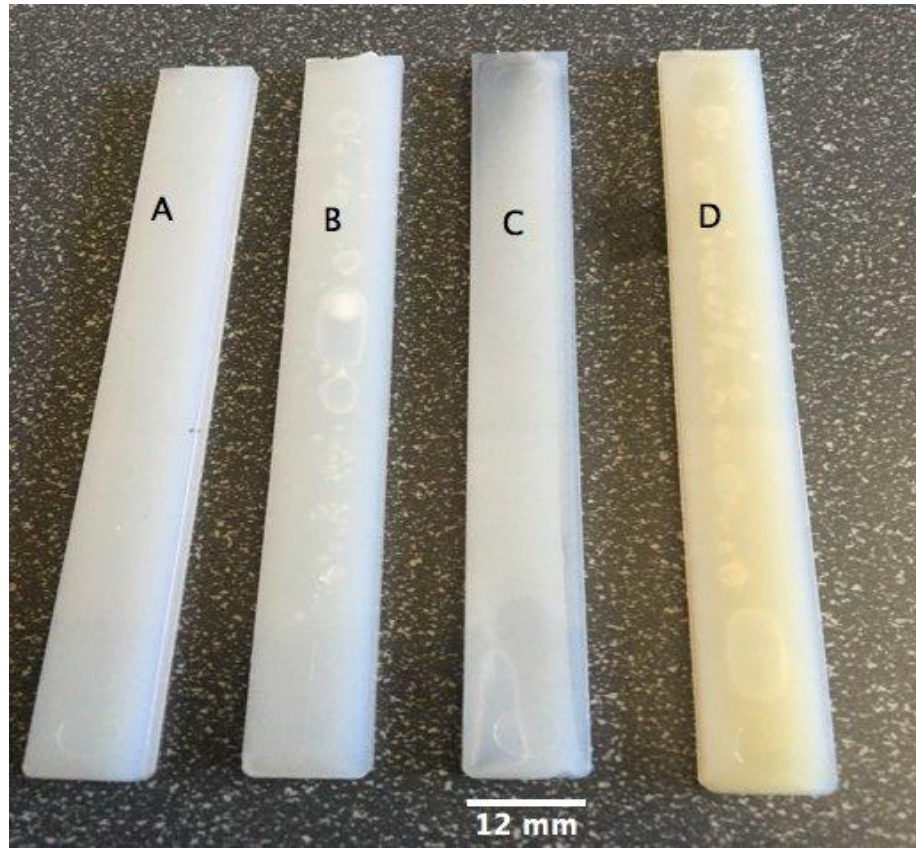
**Figure 8 - Progression of injection molded samples. A) Good sample. B) Voids. C)**

**Burn marks. D) Thermal discoloring**

**Table 7 - Formulations made for injection molding**

| Batch ID | Filler 1: (wt. %) | Filler 2: (wt. %) | Nylon (wt. %) | GF (wt. %) |
|----------|-------------------|-------------------|---------------|------------|
| MIM-Nylon | - | - | 100% | - |
| MIM-1 | Translink 445: 15% | - | 70% | 15% |
| MIM-2 | XP15-0621-A: 15% | - | 70% | 15% |
| MIM-3 | XP15-0831: 15% | - | 70% | 15% |
| MIM-5 | XP15-0721: 15% | - | 60% | 15% |
| MIM-6 | XP15-0621: 15% | - | 70% | 15% |
| MIM-7 | XP15-0621-A: 7.5% | XP15-0831: 7.5% | 70% | 15% |
| MIM-8 | - | - | 70% | 30% |

## 2.3    Characterization Techniques

The tests conducted on the specimens, the properties obtained from each test, and the corresponding testing standards followed are shown in Table 8. In addition to these tests, SEM (scanning electron microscopy) was used to study the microstructure of the composites at different magnifications.

**Table 8 - Characterization techniques used with relevant testing standards**

| Test | Properties obtained | Testing Standard [ASTM 2017] |
|---|---|---|
| Tensile | Tensile Strength, Tensile Modulus, Strain at break | ASTM D638 |
| 3-point bending | Flex Strength, Flex Modulus | ASTM D7264 |
| Izod impact | Impact Strength/ Unit Area | ASTM D256 |
| Izod notched impact | Notched Impact Strength | ASTM D256 |
| Water displacement | Density | ASTM D792 |
| Mold Shrinkage | Shrinkage after 24 & 48 hours in all 3 dimensions | ASTM D955 |
| HDT | Heat deflection temperature at 1.82 MPa | ASTM D648 |
| TGA | TGA mass degradation curves | ASTM E1131 |

In this chapter, the materials used are presented alongside with the fabrication and characterization techniques utilized. The next chapter presents and discusses the mechanical properties of the composites made using lab scale fabrication techniques.

# CHAPTER 3.  DETERMINATION OF PROPERTIES OF COMPOSITES MADE USING LAB-SCALE INJECTION MOLDING

## 3.1  Introduction

The objective of the chapter is to investigate the properties of nylon composites as a function of kaolin content, particle morphology and treatment, as well as any potential synergy between composite constituents. Samples were made using the lab-scale micro extruder and injection molding unit discussed in chapter 2. Properties were tested using the characterization techniques highlighted previously. The properties investigated were tensile modulus, strength, strain at break, flex modulus and strength, impact and notched impact strength, certain thermomechanical characteristics, and density. The purpose of these tests was to tie the performance of kaolin composites to particle interactions within the matrix and relate it to the kaolin properties outlined earlier.

## 3.2  Mechanical Properties

Figure 9 shows the effects that sample composition has on the properties of micro injection molded samples. The mineral type and weight percentage used are indicated in the specimen naming scheme. If glass fiber and mineral are used, the mineral weight percentage is shown first followed by that of glass fiber. A blend composition is also tested and contains 15% of each of the 0621 and 0831 minerals.   The results are shown as mean +/- standard deviation from 5 test samples per batch. Pure nylon and unfilled 30% glass fiber composite are used to benchmark improvements associated with mineral added.
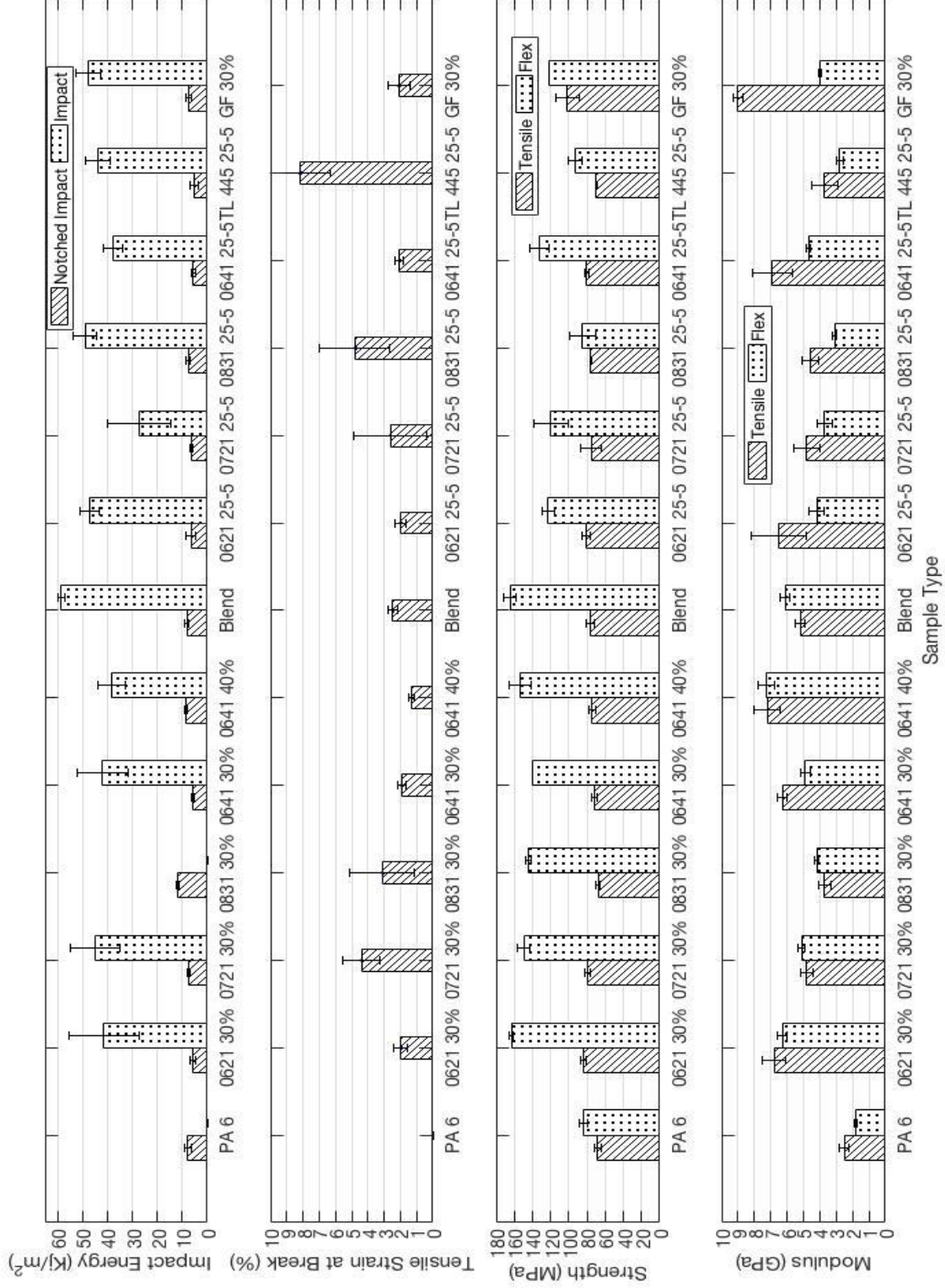
**Figure 9 – Mechanical properties of mIM samples**

Pure nylon and composites containing 0831 kaolin did not break in impact testing as their impact strength exceeded the capacity of the test frame. This is indicated by an empty bar on the graph. Nylon and composites containing GF did not break in flexural testing, the flexural strength for these samples is taken at yield. Tensile strain at break is shown as an empty bar for pure nylon due to substantial necking during testing.

There are several particle characteristics or processing conditions that can be fine-tuned to increase the strength and stiffness of a discontinuously reinforced composite at a given wt% loading. These characteristics include the intrinsic modulus of the reinforcing particle and the particle's alignment along the applied load direction, an increase of either or both will result in an increase of the both the modulus and the strength. Furthermore, the particle-polymer interfacial interactions, which are a result of the surface chemistry and size of the particles, dominate the strength of the composite as the stronger the interactions are, the more efficient is the load transfer from the polymer to the load carrying reinforcement particle.

As all testing coupons contain kaolin and are manufactured under similar conditions, it is expected that the particle modulus is more or less the same throughout the various different composite specimens made and tested in this study. This assumes no large stiffening effect on the intrinsic particle modulus due to its size, as for instance nanoparticles behave when compared to micro particles. Since all kaolin types used are within a comparable range of particle size and aspect ratios, this assumption is reasonable. Therefore, changes are mainly attributed to differences in alignment and interactions between the matrix and the particles due to differences in morphology and surface modification. It is known that there is a positive relation between aspect ratio and elastic

modulus of the composite in flake and fiber reinforced composites [Tandon and Weng 1984]. This increase can be attributed to a more uniform transfer of stresses between the matrix and filler due to the increased contact in the direction of alignment along the axis of the particle. Mallick explains a model of load transfer between the matrix and discontinuous reinforcement in the form of shear stresses at the interface [Mallick 2008]. These stresses originate at the edges of the reinforcement particles (where shear stress is maximum) and build up towards the center until maximum load carrying is reached (where shear stress drops to zero). The higher the aspect ratio, the shorter is the load transfer length needed to build up stresses, and therefore, the larger the portion carrying maximum stress.

This effect was quantified by Cox by including a modulus reduction factor (MRF) in the rule of mixtures [Cox 1952]. The MRF approaches unity with higher aspect ratio, stronger reinforcement-matrix interface, greater particle alignment, and lower particle separation distance. A stronger interface can be achieved through the application of surface treatment to the particles. Particle alignment and separation can be attributed to mineral dispersion within the matrix. Svehlova and Poloucek have shown that a better filler dispersion leads to a greater modulus [Svehlova and Poloucek 1987]. This development is explained by the percolation theory described by He and Jiang [He and Jiang 1993]. Around each filler particle, there exists a matrix zone affected by a stress concentration. When the distance between particles is small, these stress affected zones percolate into a network through which stress can efficiently travel from one particle to the next. For a constant filler mass percent loading, a smaller well-distributed particle will result in a larger volume being affected by these percolation networks. Therefore, an inverse relation between particle size and modulus and strength is expected. However, special

consideration needs to be given to agglomeration at very fine particle sizes. This is especially more pronounced for high aspect ratio plates like minerals, where the larger area of contact promotes agglomeration, and higher mass percent loading, where particles are more likely to attract each other. Agglomeration adversely affects dispersion and therefore reduces the modulus.

Both modulus and strength depend on effective stress transfer from the matrix to the particles, and from one reinforcement particle to the next. It is worth noting though that modulus measurements are taken at lower stress values (0.001-0.003 strain as specified by ASTM standards). At the lower stresses associated with these strains, stress concentrations introduced by the particles are not a significant source of weakness. As a result, it is expected that improvements in modulus surpass improvements in strengths due to that effect. This effect becomes more significant at higher mass percent loading. In addition, agglomerates at higher mineral content act as weak points that effect strength. Another effect relevant to tensile strength relates to the concept of blocking area. Small, well dispersed-particles act as a barrier to diffuse strains and crack propagation in the matrix. The smaller that particles size is, the higher the blocking area is for a given mass fraction due to their surface area to volume relationship. It is then expected that smaller particles result in higher tensile strength. This effect is explained by Vollenberg [Vollenberg 1987], Kinloch [Kinloch et al. 1985], and Adams [Adams 1993].

Impact strength decreases with the addition of kaolin and drops more for larger and higher aspect ratio particles compared to smaller and lower aspect ratio particles. This effect can be explained by multiple mechanisms. First, the addition of kaolin decreases the mobility of polymer chains [Mareri et al. 1998]. This decreases their ability to adapt to

30

sudden deformation and makes them more brittle. A second mechanism may be that the introduction of kaolin particles produces a stress concentration where cracks can initiate [Mareri et al. 1998]. Finite element simulations were used by Riley to calculate the stresses around elliptical inclusions in polymers. It was found that high axial ratios are associated with high stresses around the sharp edges [Riley et al. 1990]. These results can be expanded to conclude that high aspect ratios produce higher stress concentrations in the polymer. When this study was replicated for stresses around a crack as it approached a circular inclusion (corresponding to low aspect ratio particles), the stress around the crack fell dramatically as the crack coalesced around the inclusion [Riley et al. 1990]. Such results indicate that low aspect ratio particles are effective at retarding cracks through blocking mechanisms [Cook et al. 1964]. This allows us to revisit the concept of blocking area, the third mechanism, that can explain the adverse effect large particles have on impact strength. Smaller particles are more effective at blocking cracks due to their higher blocking area as explained earlier, hence, there is an increase in impact strength with decreasing particle size.

Dispersion and agglomeration are also noteworthy. For higher aspect ratios and higher mass fractions, agglomeration can significantly reduce impact strength [Svehlova and Poulocek 1987]. These observations are in line with Griffith's fault theory. According to Griffith, a large particle is a weak point that decreases the energy required for a composite to fracture [Mareri et al. 1998]. These stress concentrations decrease the energy required to propagate the crack through the matrix [Adams 1993]. Nakagawa and Sano have shown that the presence of fine particles dispersed within the matrix makes plastic deformation easier [Mareri et al. 1998]. Hence, in a composite where fillers are fine and well dispersed,

31

polymer chains can absorb more energy plastically and higher energy will be required to form a crack around the particle.

By looking at mineral-only containing composites (30% loading) a direct comparison between mineral properties can be established. Out of these composites, those with mineral 0621 showed the highest strength and modulus properties. The modulus of nylon increased by 1.7 and 2.7 times for tensile and flex testing modes, respectively. The tensile and flex strengths increased by 30% and 100%. The tensile modulus was within 25% of the glass fiber-only composite. It can be hypothesized that the 0621 mineral, giving composites with highest stiffness and strength, has a high aspect ratio and good dispersion. The 0641 mineral differs from the 0621 mineral in surface treatment, which produces a couple of differences in trends. It can be noted that compared to 0621 mineral sampes, 0641 mineral samples have a comparable tensile modulus but performs worse in terms of strength and impact. It is then likely that the surface treatment applied to the 0621 mineral facilitates more homogeneous dispersion and results in fewer agglomerates as explained by the mechanisms highlighted earlier. Considering the effect of increasing the wt% of the 0641 mineral from 30% to 40% the hypothesis is supported. The wt% increase resulted up to 50% increase in tensile modulus, as predicted by the rule of mixtures and percolation theory. However, the corresponding increase in tensile strength was only about 10%. The impact strength dropped with increasing the wt% of the mineral. It is likely that stress concentrations from agglomerates caused these effects.

Conversely, addition of the 0831 mineral results in opposite trends. Compared to the 0621 mineral, the 0831 mineral improved the modulus and strength of nylon by only 50%. However, its impact performance was remarkable. Like pure nylon, the composite

containing the 0831 mineral did not break in regular impact tests and produced comparable impact energy value in notched impact tests. It can be hypothesized that the 0831 mineral has a low aspect ratio and good dispersion.

Addition of the 0721 mineral produces an interesting combination of properties. It surpasses the performance of the 0641 and 0831 minerals in strength, and falls within 10% of the strength of the 0621 mineral composites. The tensile modulus is approximately 35% lower than that of composites containing the 0621 mineral, but is more than 25% higher than of those containing the 0831 mineral. It surpasses the performance of the 0641 mineral reinforced composites in terms of flex modulus. While keeping the good strengthening properties, the impact strength stays relatively high. It is only second to that of the composites containing the 0831 mineral (which did not break), and is 10% and 50% higher than that of the 0621 mineral reinforced composites in impact and notched impact respectively. From these results, a picture can be built that the 0721 mineral has a low to midrange aspect ratio but benefits greatly from good dispersion effects. There is a stiffening effect due to the aspect ratio and stiffness of the particles that, while not as great as that of the 0621 mineral, is better than that of the 0831 mineral and is almost twice of the tensile modulus of pure nylon. But, the main increase in strength and impact is due to mechanisms of low stress concentrations and good percolation as highlighted earlier. It is expected that the 0721 mineral has the lowest particles size. This, while very desirable, makes processing of the 0721 mineral harder as special conditions regarding agglomeration need to be considered to harbor these benefits.

Generally, the mineral containing composites exhibited a good correlation between tensile and flex modulus. The exception to this is the 0641 mineral, which performs

noticeably better under tension. This behavior is also seen, to a much higher degree, in the 30% GF control batch.

The addition of glass fibers to the mineral/nylon composites, produced similar trends. A couple of differences to be highlighted include that the absolute values are lower for the 25/5 GF/mineral formulation than for the 30% mineral only composites for all minerals. Since GF are stiffer than mineral particles an opposite trend is expected. Furthermore, the standard deviation is higher, especially for the 0641 and 0621 mineral composites. This can be understood from the perspective of dispersion and fiber alignment within the matrix. Glass fiber is larger in size than the mineral fillers. As a result, it is harder to evenly disperse and align. For micro scale fabrication, this effect can be prominent. This can also explain the higher standard deviation as differences in alignment between test samples will yield different results. Lastly, the composites perform better under tension. As fibers are generally strong along their axis, they are expected to have higher enhancements in tensile properties over flexural.

From these patterns, it can be established that stiffness and strength follow a trend opposite to impact energy. It is then of practical importance to develop stiff composites without compromising impact, a task not usually achievable as one is enhanced at the expense of the other. To achieve this goal of property balance, it is noteworthy to consider a blended batch made from equal parts of the 0831 and 0621 minerals considering that addition of each mineral alone enhances a different property. Based on the results of mineral only reinforced nylon, it has been established that the 0621 mineral greatly improves stiffness and strength, while the 0831 mineral has better impact characteristics. It is then expected that addition of both the 0831 and 0621 minerals would drive their

opposing properties down to an average of the two. Nevertheless, when compared to the 0621mineral/nylon composite, the drop-in modulus and strength was marginal. Flex strength, tensile strength, and flex modulus all decreased by 5% or less whereas the Tensile modulus decreased by 20%. In terms of impact strength, the blend's impact was within 25% of that of the 0831 mineral/nylon composite in notched impact strength, but significantly surpassed that of the 0621 mineral/nylon composite by 50% for impact and notched impact energies. This implies a synergistic effect between the mineral fillers. A look at percolation theory can explain such synergy. The presence of lower aspect ratio particles can fill in the gaps between the higher aspect ratio ones, improving the percolation between them. Thus, it can be seen that the high aspect ratio mineral first disperses within the matrix, which is easier with half the amount of mineral, and creates a stiffening skeleton within the matrix. The lower aspect ratio mineral then embeds itself between the gaps in that skeleton enhancing the percolation network and greatly improving stress transfer.

### 3.3    Thermomechanical Properties and Density

The density of the composites is of importance to this study. Ideally, a high strength to weight ratio is desired. This can be achieved by minimizing the density of the composite for a given strength. The heat distortion temperature (HDT) is a measure of the dimensional stability of the composites. A higher heat distortion temperature is indicative of less deformation with increases in temperature under a constant load. This is desirable in automotive applications for under-the-hood components that experience an increase in temperature while the vehicle is in operation. Table 9 shows HDT and density measurements for representative composite formulations. HDT testing was conducted at

1.82 MPa as specified by ASTM standards. The values reported are the average of five measurements for the density and the midpoint of two measurements for HDT.

The first column shows the density of the composites measured by water displacement. Comparing the densities of the composites, no significant difference was found. All density measurements overlapped considering the standard deviation. The datasheet densities of glass fibers and mineral fillers are 2.62 and 2.61 respectively. Since their densities are similar, no adverse effect on weight is present.

**Table 9 - HDT and density**

| Specimen Type | Density (g/mL) | HDT ($^{\circ}$C) |
|---|---|---|
| GF 30% | 1.43±0.06 | 176.0±4.5 |
| 0621 25-5% | 1.39±0.02 | 148.8±0.9 |
| 0641 25-5% | 1.42±0.08 | 141.3±2.0 |
| 0641 30% | 1.39±0.01 | 134.2±0.3 |
| Blend | 1.36±0.07 | 119.9±0.96 |
| 0721 25-5% | 1.38±0.04 | 116.7±6.4 |
| TL 445 25-5% | 1.36±0.03 | 101.0±5.4 |
| 0831 25-5% | 1.37±0.05 | 96.1±4.1 |

HDT results are shown in the second column. HDT values are arranged form high to low. Glass fiber composites exhibited the highest distortion temperature. Following that, minerals that showed the highest improvement in stiffness also showed the highest HDT values. From this, it can be hypothesized that HDT not only depends on the dissipation of heat in the composite, but also on the initial stiffness of the composite in question. For automotive manufacturing applications, it is desirable that composites have a high distortion temperature. In addition, it is desirable that connected or interacted components have comparable distortion temperatures so that they can deform uniformly with temperature.

The thermal stability, ash content, and moisture content of the composites were investigated using thermogravimetric analysis (TGA). Table 10 shows the results for composites reinforced with both kaolin and glass fibers, neat nylon, and as received nylon pellets (both dried and un-dried). Each column presents the mass loss in wt% between 100 ºC and 600 ºC at 100 ºC intervals. T-50 and T-max are the temperatures at which 50% mass loss and maximum loss are reported respectively. At 100 ºC and 200 ºC most mass loss can be attributed to moisture. Un-dried nylon had 0.25% moisture. The drying process was effective at removing the moisture as shown by the TGA results. For composites containing glass fiber, an additional source of mass loss is the sizing on the fiber coating.

The onset of thermal degradation is between 400 ºC and 600 ºC. At T-max, maximum mass loss is reached and ash content can be measured. Higher T-max and T-50 measurements indicate higher thermal stability. Degradation of polymers is characterized by the presence of low molecular weight polymer chains which drive the mass loss temperatures down [Iwaya et al. 2006]. Compared to as received nylon pellets, processed

nylon showed only a 2% drop in T-50. This indicates that no significant degradation occurred during processing. The addition of kaolin and glass fibers increased T-max and T-50 further due to their inorganic structure being more thermally stable. The mass loss at 600 °C can be used to estimate the ash content. It can be seen that nylon degrades almost completely. The addition of kaolin and glass fiber increased the ash content. When comparing glass fiber composites with the composite containing both 0641 mineral and glass fibers, one can see that the composite with the mineral has a higher ash content. It can be concluded that kaolin is more thermally stable than glass fibers.

**Table 10 – Thermal degradation of composites based on TGA**

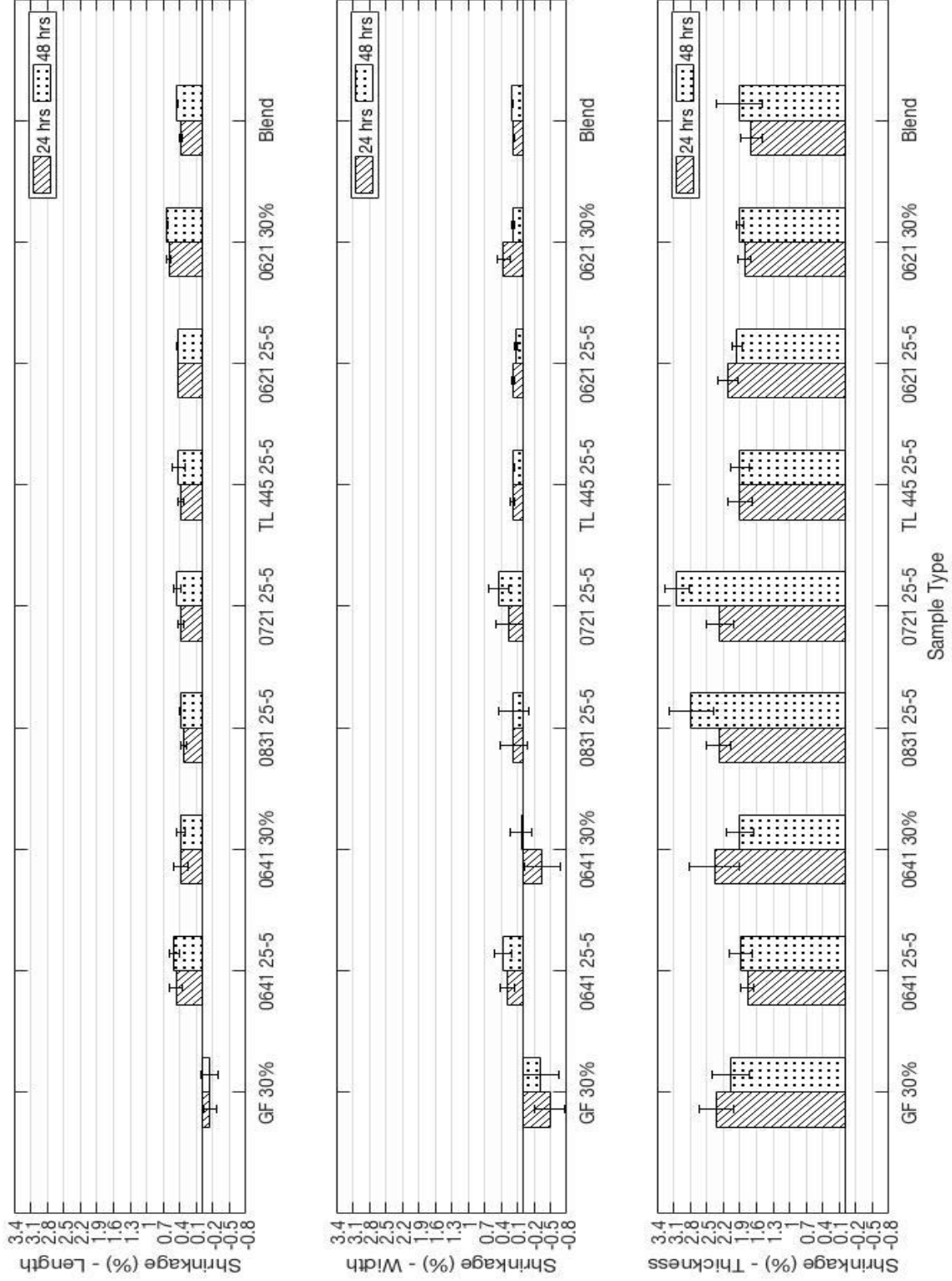| Sample ID | 100 °C [% ML] | 200 °C [% ML] | 400 °C [% ML] | 500 °C [% ML] | 600 °C [% ML] | T-50 [°C] | T-max [°C] |
|---|---|---|---|---|---|---|---|
| 0641 25-5% | 0.03 | 1.38 | 8.18 | 67.4 | 76.18 | 459 | 596 |
| 30% GF | 0.31 | 1.71 | 9.66 | 66.95 | 88.27 | 454 | 590 |
| 0641 40% | 0 | 0.07 | 5.02 | 58.04 | 69.7 | 459 | 590 |
| Nylon 100% | 0 | 0.83 | 14.53 | 92.05 | 94.6 | 425 | 568 |
| Dried NP | 0 | 0.15 | 14.96 | 90.26 | 96.99 | 435 | 528 |
| Un-dried NP | 0.25 | 0.19 | 14.56 | 88.02 | 95.18 | 434 | 585 |

**Figure 10 – Mold shrinkage in L, w, t dimensions**

Figure 10 shows the results of the mold shrinkage measurements. The shrinkage in length (parallel to molding direction), width, and thickness dimensions is shown. This is done by measuring the dimensions of the specimens along the corresponding directions 24 and 48 hours after molding, and calculating the shrinkage with respect to the mold dimensions. The values reported are the average of measurements made in five specimens for each composition. Shrinkage is indicated by a positive value, and expansion is indicated by a negative one.

Shrinkage occurs as the polymer cools down and arranges itself into a crystalline structure after molding. Reduction in crystallinity is a possible mechanism for reducing shrinkage. DSC measurements have shown that the introduction of minerals into the formulation reduced the crystallinity of the composite. This is supported by reduction in shrinkage in the thickness dimension. However, error and standard deviation for some of the samples make these results inconclusive.

Glass fiber composite are anisotropic in nature, resulting in non-uniform shrinkage behavior along the various directions. It can be hypothesized that mineral filler particles act as pin points in the matrix preventing the polymer chains from shrinking [Karian 2003]. Thus, a positive relationship is expected between filler content and shrinkage reduction as explained by this mechanism.

**3.4    SEM and Morphology**

SEM was used to investigate the dispersion state of the minerals and glass fibers within the matrix as well as failure modes of the composites. The tensile fracture surfaces were viewed after they were gold coated.
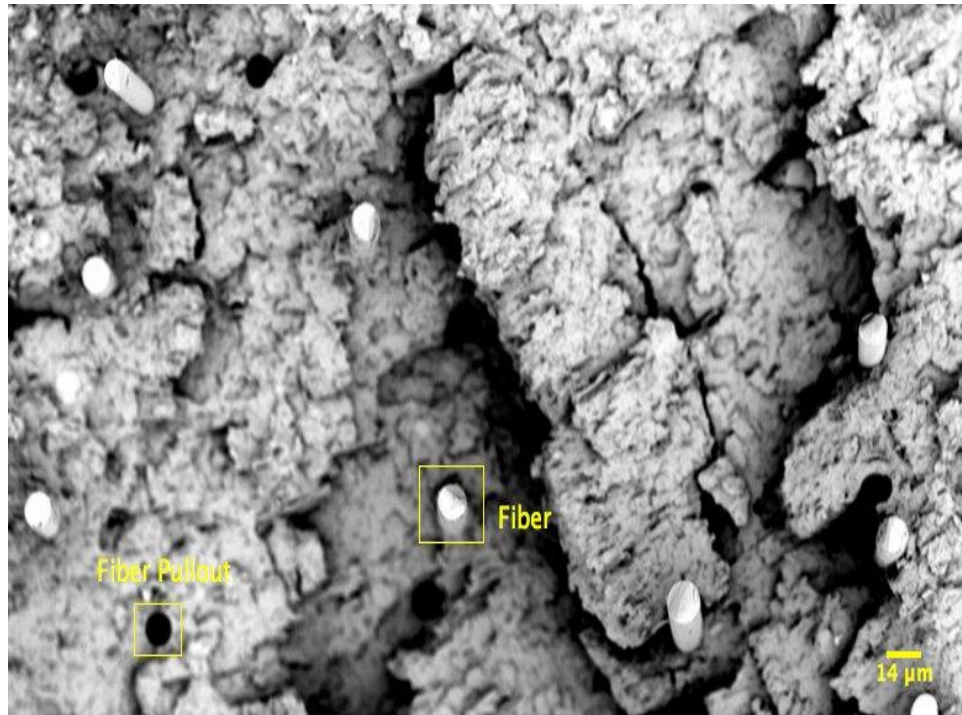
**Figure 11 - SEM of 25/5/70 wt% 0621/GF/Nylon composites**
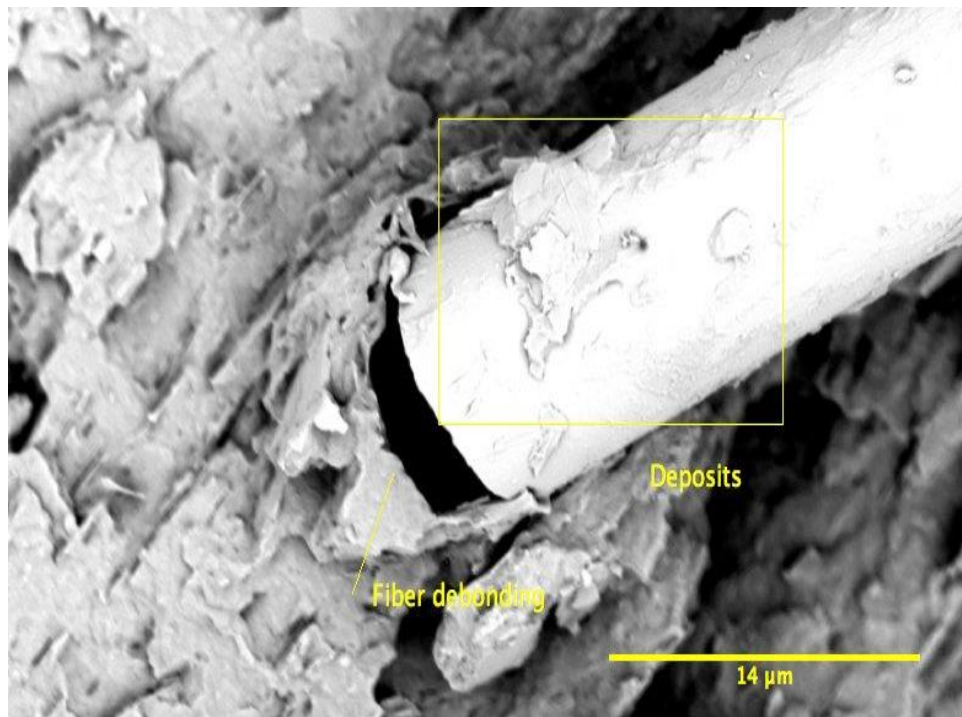


**Figure 12 - SEM of 25/5/70 wt% 0621/GF/Nylon composites (higher magnification)**

Figure 11 shows the SEM fracture surface of 25/5/70 wt% 0621/GF/Nylon composites. Multiple failure modes can be seen. Fiber pullouts are present indicating fiber-matrix de-bonding. The fibers show a preference of alignment in the direction of injection; however, some fibers show angular alignment as well. Of particular interest is the highlighted fiber, which is shown in higher resolution in Figure 12. The fiber indicated is on the onset of break with some de-bonding present. Polymer residue or mineral deposition on the fiber surface can also be seen. This would indicate an affinity between the fiber and the mineral. A good mineral coating on the fiber can potentially increase fiber adhesion and improve the interfacial strength. As discussed earlier, this increases the modulus and strength.
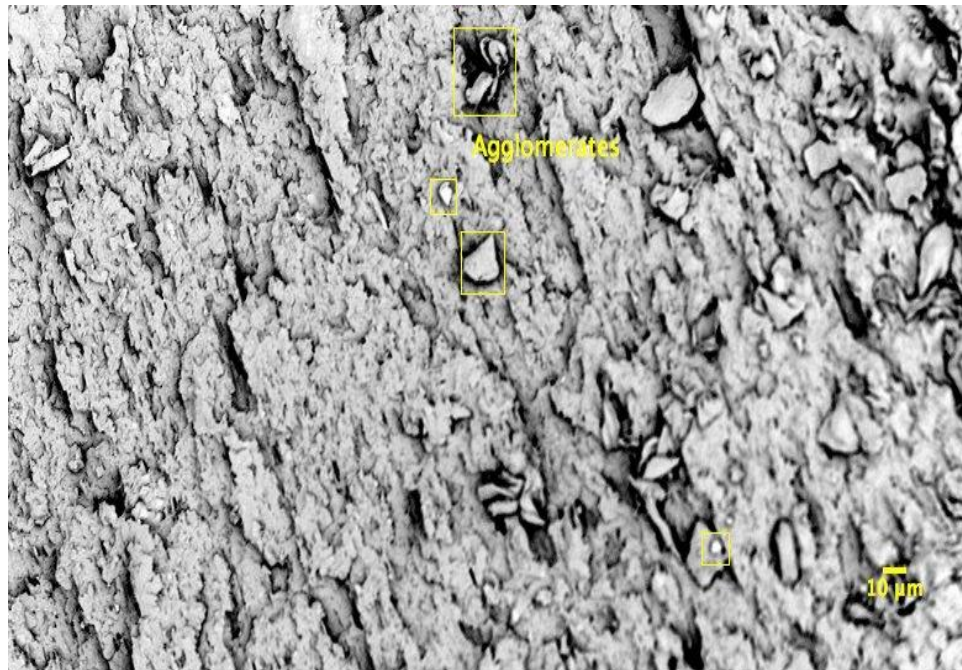


**Figure 13 - SEM of 30/70 wt% 0641/Nylon composites showing agglomerates**
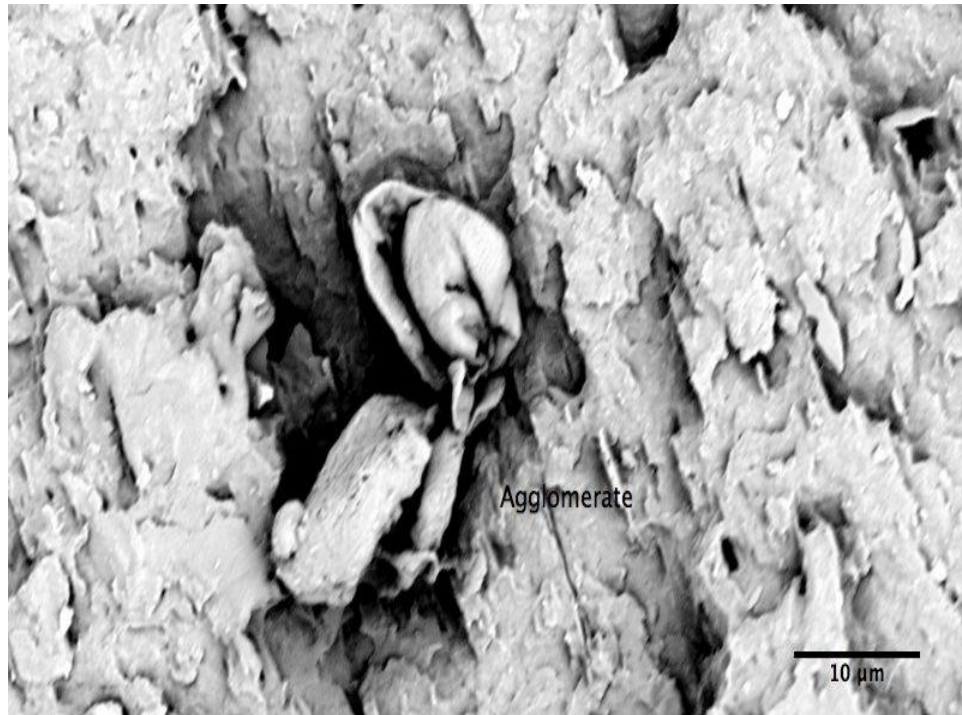
**Figure 14 - SEM of 30/70 wt% 0641/Nylon composites (higher magnification)**
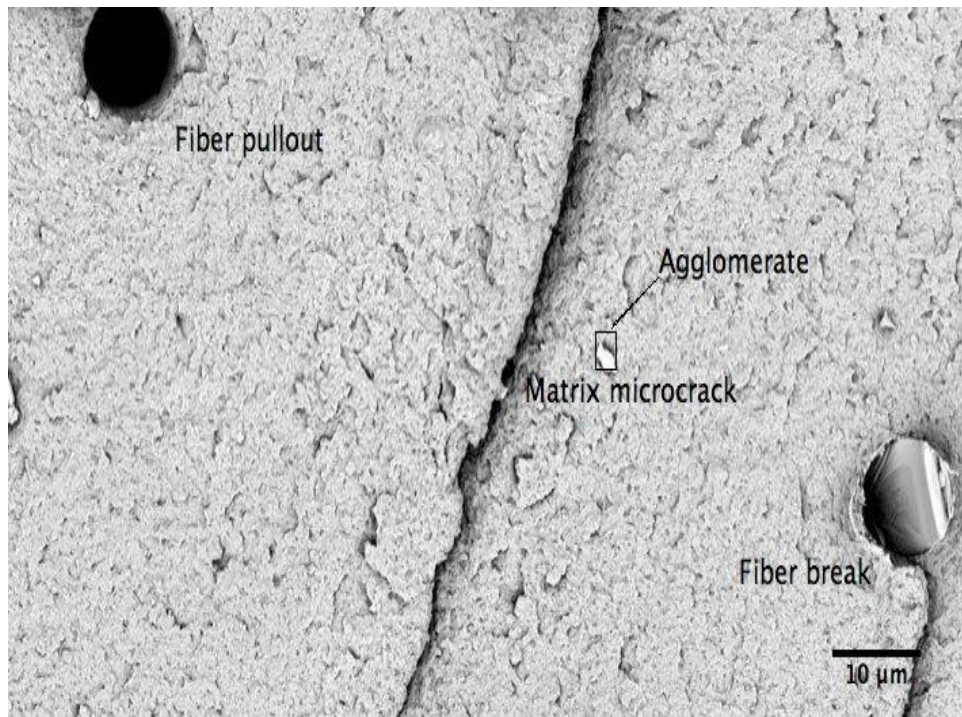


**Figure 15 - SEM of 25/5/70 wt% 0721/GF/Nylon composites**

Figures 13 and 14 are SEM micrographs of the fracture surface of 30% 0641 mineral/nylon composites. Mineral agglomerates, which as discussed can act as stress concentration points, can be seen. Figure 15 shows the fracture surface of 25/5/70 0721mineral/glass fiber/nylon composite. It is first noticeable that the fracture surface is smoother than that of the 0641 mineral composite indicating that more energy is required to break these composites. Three modes of failure can be identified in the SEM micrograph. A crack in the matrix is seen towards the middle. Fiber pullout and fiber breaking are also seen. Furthermore, mineral agglomerates are present to a lesser extent compared to the composite containing only the 0641 mineral. The agglomerates are also smaller in size. Figure 16 shows the SEM fracture surface of 30% GF/nylon composite random distribution of the glass fibers can be seen.



**Figure 16 - SEM of 30/70 wt% GF/Nylon composites**

## 3.5    Conclusions

The presence of kaolin minerals alters the properties of the nylon matrix. The mineral characteristics that have a strong effect on the properties of the composites are the morphology including shape, size and aspect ratio, the surface modification, and the amount (wt%) used. A higher aspect ratio mineral can facilitate better stress transfer and improve the modulus and strength. The addition of mineral decreases the mobility of polymer chains and thus decreases the impact strength. Low aspect ratio minerals, however, were found to hedge that reduction. The effect of aspect ratio on the impact and strength is not the same. A balance between stiffness improvement and impact reduction is sought after. Synergistic effects between fillers were found that improved the balance of properties. Good particle dispersion is desirable for all properties. Small particle size is associated with good dispersion. However, special considerations are given to agglomeration at higher mineral contents.

No significant changes in density were recorded among the various composites. HDT tests showed a correlation between HDT and stiffness. Mold shrinkage results indicated anisotropic behavior for GF and a reduced shrinkage with the addition of minerals. TGA showed effective removal of moisture with the drying methods used. No effective degradation was caused by the processing of nylon. Mineral composites showed a higher ash content than glass fiber composites.

The SEM study indicated that there are multiple failure modes. The 0721 mineral composite exhibited smother surface and better dispersion compared to the 0641 one.

The next chapter discusses the properties of scale up fabricated kaolin composites and compares the trends established in this chapter to trends achieved when the manufacturing process is scaled up.

# CHAPTER 4.     EFFECTS OF SCALE-UP MANUFACTURING

## 4.1   Introduction

The objective of the chapter is to investigate the effects scale-up manufacturing has on the properties of kaolin composites. Compared to micro scale fabrication, scale-up manufacturing is done at higher volume under more aggressive mixing conditions and higher injection pressure due to the size of the machinery. Larger ASTM testing coupons with dimensions according to ASTM standards were made using macro fabrication techniques outlined in chapter 2. Properties were tested using the characterization techniques highlighted previously. The properties investigated were tensile modulus, strength, strain at break; flex modulus and strength; impact and notched impact strength; as well as heat distortion temperature and density. The purpose of these tests was to investigate the properties of kaolin composites in a controlled setting using an industrially relevant manufacturing method. Of particular interest is to determine whether or not the trends of the enhancement of the various properties are the same when composites are made using large-scale instead of lab-scale injection molding. A discussion of relevant challenges associated with scale-up manufacturing of mineral fillers will also be presented.

## 4.2   Mechanical Properties

Figure 17 shows the mechanical properties of kaolin containing composites made using the larger scale injection molding machine. The mineral type is shown on the x-axis. A constant mineral to glass fiber ratio of 15-15% is used. A composite containing equal parts (7.5% wt. of each) of the 0621-A and 0831 and 15% glass fiber was also made.
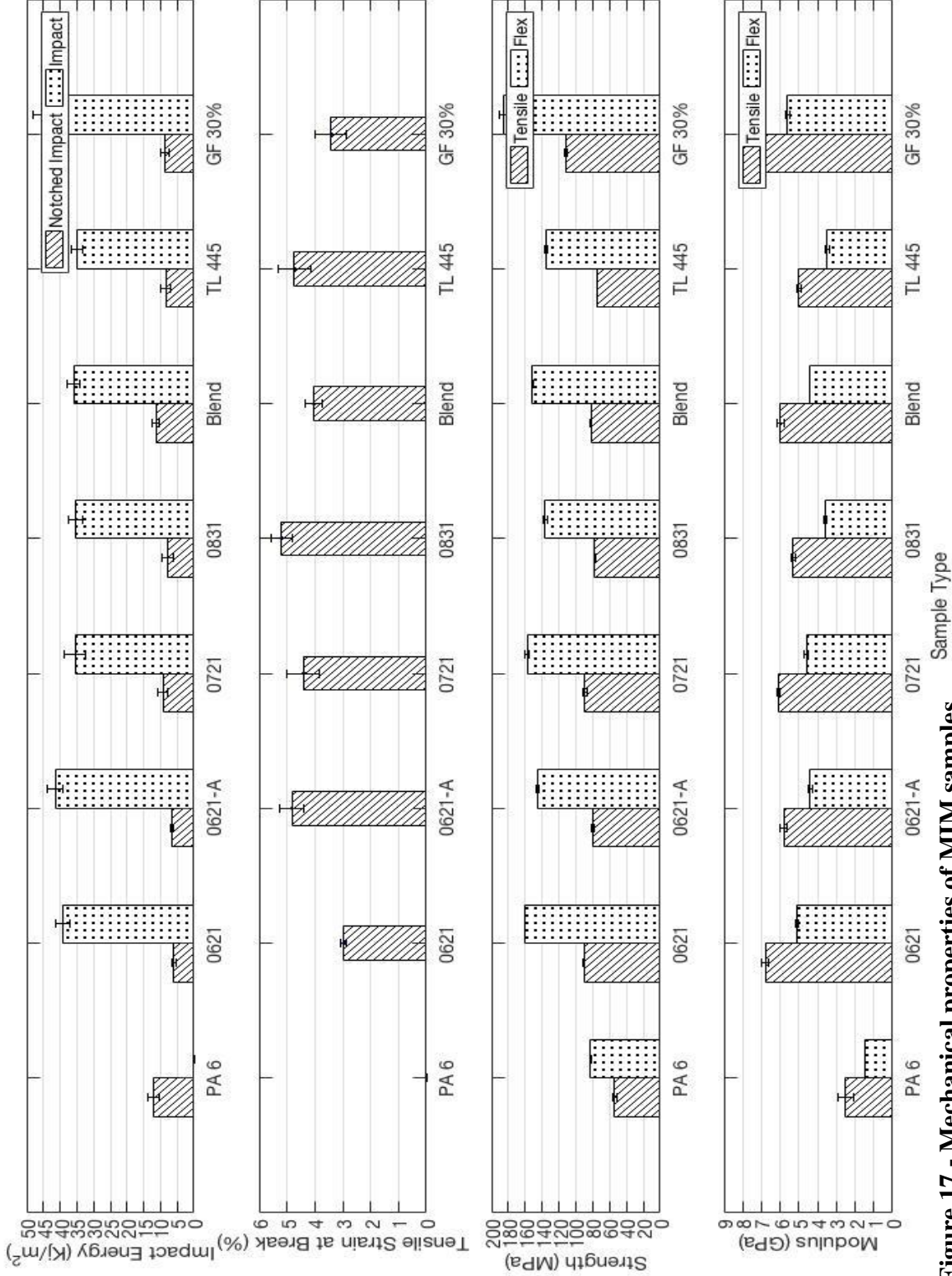
**Figure 17 - Mechanical properties of MIM samples**

Twenty testing coupons were fabricated for each composition. The first six coupons from each composition were discarded to ensure the injection molding machine had reached steady state. Seven coupons per test per composition were randomly chosen from the remaining samples. Testing coupons of compositions that did not break during testing are represented by empty bars. Pure nylon and 30% glass fiber composites are used for benchmark.

The first noteworthy observation is a substantial decrease in standard deviation, compared to the one associated with the corresponding properties of composite made using the lab-scale fabrication techniques. This can be attributed to a better control of fabrication conditions resulting in uniformity across samples. Unlike micro-scale fabrication, the coupons are manufactured in a continuous mode as opposed to smaller batches limited by the barrel size of the small compounding unit. Due to that continuous nature, the manufacturing conditions are standardized for all coupons made for each composition.

The injection capabilities of the machine also affect the properties of the composites. Higher injection pressure leads to better alignment of reinforcing fibers and particles [Mallick 2008]. In the previous chapter, it was discussed that sensitivity to alignment can produce significant standard deviation and overlapping error bars among the various composites and a reduction in flexural properties. To investigate this, the properties of 30% GF composites made by the two techniques are compared. Compared to mIM, the flexural modulus increased by 40%. This increase can be attributed to higher degree of fiber alignment along the injection molding direction. This is in line with percolation theory highlighted by He and Jiang [He and Jiang 1998] which is explained in chapter three.

Scaled up manufacturing also results in better dispersion. Screws used on larger machines have a greater length and diameter compared to tabletop compounders used in micro-scale fabrication. This allows for a larger mixing region as well as a longer helix path taken by the polymer as shown by Figure 18. As a result, the composite can be sufficiently mixed in shorter periods of time. This not only decreases thermal degradation (due to shorter mixing times), but also better distributes any particles within the polymer matrix. Higher shear capabilities are also more effective at breaking up agglomerates [DuPont 2001]. Better fusion can also be achieved with better mixing as it promotes contact between the matrix and the reinforcement. Special consideration needs to be taken, however, to fiber breakage under more aggressive mixing conditions.
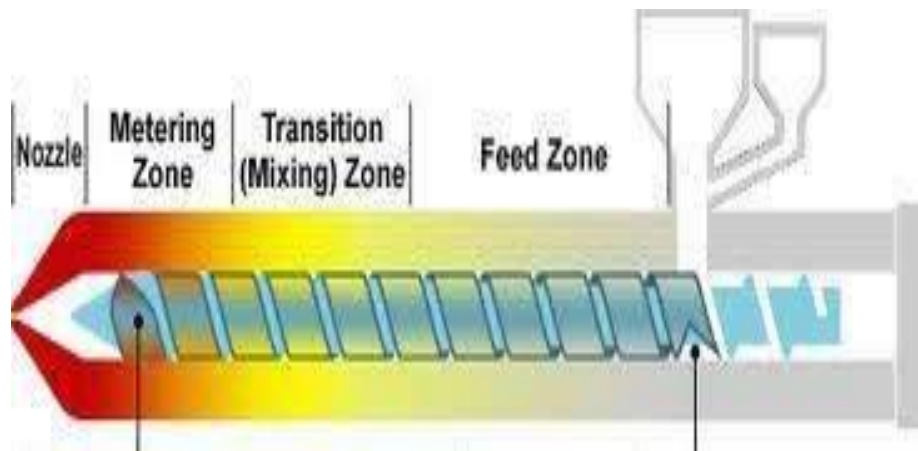


**Figure 18 - Injection molding screw regions [DuPont 2001]**

It is noteworthy that the trend for the mechanical properties enhancement of the composites is the same regardless of the manufacturing method used to make the composites. The inclusion of high aspect ratio particles, such as the 0621 mineral, best improved the stiffness and strength of the composite. Better stress transfer, as in the model shown by Mallick [Mallick 2008] and Cox [Cox 1952], explains this increase. It can be

noted that when a different surface treatment is used within the same family of morphology, for example the 0621-A mineral compared to 0621, is used then the modulus and strength drop. It can be inferred that the 0621 mineral has a superior surface treatment. When considering impact results, the results are not conclusive as there is an overlap of the standard deviation in unnotched impact energy values due to the addition of glass fiber to the formulation. Notched impact results are more conclusive and can be used to compare the minerals. The composites containing the 0831, 0721 minerals, and the mineral blend exhibited higher impact than the composites containing only the 0621 mineral. This supports the hypothesis that the mechanism for enhancement of impact is opposing the one for the enhancement of the modulus. The 0721 mineral produces desirable qualities in both areas due to the effects of particle size.

Overall, there is trade of between enhancement of stiffness and impact energy. The inclusion of low aspect ratio particles, such as the 0831 mineral, does not increase the stiffness of nylon as much as high aspect ratio particles do, but it greatly hedges reductions in impact. On the other hand, substituting a portion of glass fibers with the high aspect ratio 0621 mineral only reduced stiffness by 12% compared to that of composites with glass fibers only, but the impact strength dropped further. Blending both minerals produced a synergistic effect explained by the percolation theory. The blend formulation showed a mild 10% reduction in stiffness compared to the 0621 mineral composite, but maintained the highest notched impact strength among all mineral formulations. It is worth mentioning that the test mineral formulation outperformed the commercially available TL 445 mineral, in all categories. This indicates that the minerals investigated in this study exhibit superior morphology and surface treatment.

Comparing notched and unnotched impact results, one obtains an insight into the sensitivity of the composites to defects. In the unnotched case, glass fiber composites showed the highest impact energy absorption. However, when notched impact was considered, glass fiber composites showed the most severe drop by 80% in impact strength This is compared to 70% drop for the blended mineral formulation. According to Griffith's failure theory, there are two energies associated with the failure of a composite. These are the energies needed to create a crack site and the elastic energy released as the crack propagates through the material. When the energy released is at least equal to the energy required to generate a crack, crack propagation will occur and the composite will fail. Thus, from the lower notched impact energy it can be hypothesized that cracks propagate more easily in glass fiber composites, compared to low aspect ratio mineral composites.

This drop can be described by two mechanisms. First, higher elastic strain energy can be stored in glass fibers due to their high stiffness. When the crack propagates, this energy is released making initiation of new cracks easier, in line with Griffith's theory. The second mechanism is related to the finite element simulations performed by Riley that were discussed in chapter 3. It was shown that low aspect ratio particles merge with cracks effectively blocking their propagation. It can be hypothesized that the opposite effect is true for high aspect ratio reinforcement such glass fibers. As a crack approaches a fiber, it cannot break and cross through the fiber but has to go around or along the fiber de-bonding the fiber from the surrounding matrix. Depending on the relative strength of the fiber-matrix bond strength compared to the blocking effect of minerals, this can decrease the energy needed to create fracture surfaces in Griffith's model. It can then be anticipated that, depending on the strength of the fiber-matrix interface, glass fiber composites can

have a strong initial resistance to impact due to their good energy absorption. However, at the onset of cracking (or the intentional introduction of a defect such as in notched impact) their impact resistance drops due to ease of crack propagation. A similar effect could also be inferred for very high aspect ratio particles.

## 4.3    HDT and Density

Density and HDT tests were conducted for the composites made using the scale-up fabrication. The results are shown in Table 11. A constant mineral to glass fiber ratio of 15-15% is used throughout. For the GF-only batch, 30 wt.% is used. Equal parts (7.5% wt. of each) of minerals 0621-A and 0831 added to 15% glass fiber are used in the blend batch. The first column shows the density of composites measured by water displacement. The density of nylon was obtained from the material datasheet. Comparing the densities of the composites, no significant difference was found. Like the results from micro scale fabrication, it can be inferred that the densities of glass fibers and the mineral fillers are similar. No adverse effect on weight is presented by subsisting glass fibers with minerals. Compared to lab-scale measurements, the reduction in standard deviation and difference between samples in measured density indicates consistent formulation and processing conditions. This is associated with more controlled fabrication conditions in scaled-up manufacturing.

HDT results are shown in the second column. HDT values correlate to the stiffness of the reinforcements. High stiffness glass fiber composites exhibited the highest distortion temperature. Following that, composites with similar stiffness exhibit similar HDT values.

**Table 11 - Density and HDT values for MIM composites**

| Sample Type | Density (g/mL) | HDT (ºC) |
|---|---|---|
| GF | 1.34±0.00 | 178 |
| Nylon | 1.12-1.15 [MatWeb 2017] | 79 |
| 0621-A | 1.33±0.01 | 152 |
| 0831 | 1.34±0.00 | 124 |
| TL 445 | 1.34±0.01 | 126 |
| 0621 | 1.32±0.00 | 159 |
| 0721 | 1.32±0.01 | 143 |
| Blend | 1.32±0.01 | 146 |

## 4.4 SEM and Morphology

To investigate the effect of fabrication techniques on the morphology of the composites including the dispersion and distribution of the minerals, the orientation of the glass fibers and presence of voids or other defects, SEM micrographs of the fracture surfaces of the testing coupons obtained under tensile testing are shown.
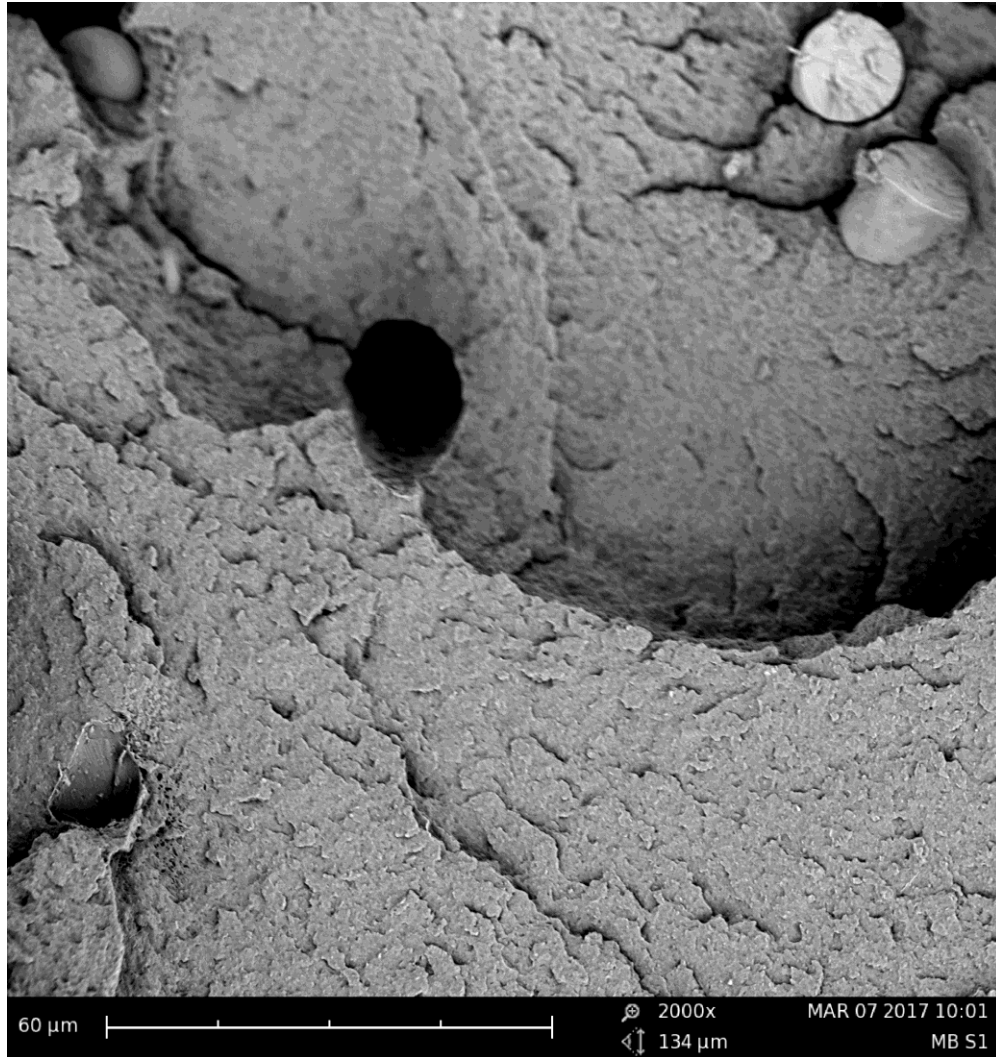
**Figure 19 - SEM of 15/15/70 wt% 0721/GF/Nylon composites**

Figure 19 shows the SEM fracture surface of the 15/15/70 0721 mineral/glass fiber/nylon composite. Lack of agglomerates at this resolution indicate that the mineral particles are well dispersed compared to the SEM micrographs of composites containing only the 0721 mineral. This is expected considering that the mixing achieved through the larger scale injection molding machine is better.

**Figure 20 - SEM of 15/15/70 wt% 0621/GF/Nylon composites**

Figure 20, shows the SEM micrograph of the 15/15/70 0621 mineral/glass fiber/nylon composite. Some mineral agglomerates or fiber glass fragments can be seen indicating that that the dispersion is more homogeneous and the agglomerates are smaller in the 0721 mineral/glass fiber/nylon composite.

**4.5    Associated challenges in scale-up fabrication**

As discussed in the previous section, aggressive mixing and injection can lead to glass fibers breakage, resulting in shorter than desired fiber lengths. This can adversely affect the modulus and strength of the composite. To overcome this effect, a side feeder can be utilized to add the glass fibers towards the end of the barrel. This decreases the amount of shear experienced by the fibers decreasing the amount of breakage. This, however, reduces the amount of mixing.

During scaled up manufacturing, a high volume of parts is produced. Therefore, a one-step compounding-molding process is highly desirable. Otherwise, the cycle time can be significantly affected. The fabrication methods utilized in this study include separate compounding and molding steps. It was attempted to premix all the composite constituents and mold them directly. However, concerns about achieving proper mixing prevented this. Solid state compounding can be utilized to effectively and quickly mix the pellets with the powders in a tumble mixer. The fibers can then to be added using a secondary feeder. When the polymer powder and mineral were mixed first, it was found that the pellets started sticking to each other and the hopper. It is hypothesized that the fine powders stick on the high surface area of the pellet, and them in turn promote the pellets to stick to each other. Premixing the powders and the glass fibers did not produce a similar effect. A side feeder can then be used to add the fiber-mineral mix.

The abrasive nature of glass fibers makes them harder to handle, store, and process. Being in powder form, mineral fillers do not pose such concerns but due to their high surface are to volume ratio they tend to form agglomerates, which are often very difficult to break down and disperse.

Blending mineral fillers can be efficiently done using a tumble mixer. It was shown that this can produce a desirable set of properties not easily achievable using single reinforcement composites. No such mixing techniques are available for fiber composites.

Shrinkage of polymers during manufacturing introduces issues of warpage in the fabricated parts. As discussed in chapter 3, introducing mineral fillers could potentially reduce the shrinkage of parts.

## 4.6    Conclusions

Scale up manufacturing affected the properties of the composites in a similar trend to lab scale fabrication. Higher injection pressure resulted in better alignment of reinforcing fibers and fillers. This led to improvements in flex modulus, as demonstrated by comparing glass fiber composites made by the two fabrication methods. Larger screw dimensions and higher mixing forces lead to better dispersion and lower the potential for thermal degradation due to shortened mixing times. Patterns on particle morphology were like the ones established using micro-scale fabrication. Higher aspect ratios resulted in higher stiffness, while lower aspect ratios better maintained impact strength. A synergistic effect between minerals the 0621 and 0831 was also observed, similar to the synergistic effects observed for the same composites made using the lab-scale technique. Glass fiber composites showed a sensitivity to defects as demonstrated by a severe drop in impact energy in notched impact tests. This may be due to easier crack propagation. A similar effect could be expected with high aspect ratio fillers.

No adverse effect on density was found when substituting glass fibers with mineral fillers. HDT tests showed patterns that correlate HDT with the stiffness of the composites.

SEM pictures show few agglomerates and good dispersion. Better mineral dispersion is seen for composites containing the 0721 compared to the 0641 mineral. Glass fibers are not fully aligned which means that the properties especially the tensile modulus can be further increased by increasing the injection pressure.

Overall, the characteristics of the minerals including morphology, surface treatment and aspect ratio facilitate their use in large scale manufacturing of nylon composites.

The next chapter will evaluate the efficiency of the reinforcing materials used through comparing the experimental data achieved to predictions from michromechanical modeling.

# CHAPTER 5.    COMPARISON OF EXPERIMENTAL RESULTS

# TO THEORETICAL PREDICTIONS

## 5.1    Introduction

It is important to benchmark experimental results against theoretical predictions and similar results found in literature. In this chapter, the experimentally determined tensile modulus is compared with the modulus values predicted by the Halpin-Tsai theoretical micromechanical model. A list of the underlying assumptions of this model are discussed. Existing experimental data found in literature are also provided for comparison. Deviations from the model will be explored and related to underlying assumptions in the model and actual fabrication conditions.

## 5.2    The Halpin-Tsai Micromechanical Model

The analysis in the chapter is modeled after the Halpin-Tsai model. The Halpin-Tsai equations are an expansion of the rule of mixtures and are commonly used to predict the tensile modulus of composites where discontinuous reinforcements are used. The first case explored here is nylon reinforced with discontinuous chopped glass fibers randomly distributed resulting in plane-isotropic lamina as shown in Figure 21. [Mallick 2008].

**Figure 21 - Randomly oriented discontinuous fiber lamina (left) vs uniformly aligned discontinuous fiber lamina [Mallick]**

The following assumptions are associated with the Halpin-Tsai model [Mallick 2008].

1.  Fiber cross section is circular

2.  Fibers are arranged in a square array

3.  Fibers are uniformly distributed throughout the matrix.

4.  Perfect bonding exists between the fibers and the matrix.

5.  Matrix is free of voids.

   In the case of glass fibers assumption one holds and assumptions two and three are associated with the manufacturing method and processing conditions. For random mixing achieved though melt compounding and low pressure injection molding, it can be assumed that these assumptions hold as well. Ideally, there should be strong interfacial strength and minimal matrix voids for assumptions four and five to hold. For a random discontinuous lamina, the elastic modulus is calculated from Equation 1 [Mallick 2008]. $E_{random}$ is the tensile modulus of the randomly oriented lamina, $E_{11}$ and $E_{22}$ are the longitudinal and transverse moduli of a unidirectional discontinuous fiber lamina shown in Figure 21. The

longitudinal modulus is the modulus parallel to the direction of alignment, and the transverse modulus is the modulus perpendicular to it. These are calculated by Equation 2 and Equation 3, respectively.

$$E_{random} = \frac{3}{8}E_{11} + \frac{5}{8}E_{22} \tag{1}$$

$$E_{11} = \frac{1 + 2\frac{l_f}{d_f}\eta_L v_f}{1 - \eta_L v_f}E_m \tag{2}$$

$$E_{22} = \frac{1 + 2\eta_T v_f}{1 - \eta_T v_f}E_m \tag{3}$$

$l_f$ is the average fiber length, $d_f$ is the diameter of the fiber, $v_f$ is the fiber volume fraction which can be calculated from the mass fraction using Equation 4, $E_m$ is the modulus of the matrix, and $\eta_L$ and $\eta_T$ are calculated by Equation 5 and Equation 6, respectively. $w_f$ is the mass fraction of the fiber, $w_m$ is the mass fraction of the matrix, $\rho_f$ is the specific gravity of the fiber, $\rho_m$ is the density of the matrix, and $E_f$ is the elastic modulus of the fiber.

$$v_f = \frac{w_f/\rho_f}{\frac{w_f}{\rho_f} + \frac{w_m}{\rho_m}} \tag{4}$$

$$\eta_L = \frac{E_f/E_m - 1}{\left(\frac{E_f}{E_m}\right) + 2(\frac{l_f}{d_f})} \tag{5}$$

$$\eta_T = \frac{E_f/E_m - 1}{\left(\dfrac{E_f}{E_m}\right) + 2} \tag{6}$$

This model can directly be applied to chopped glass fiber reinforced nylon composites. By relaxing assumption one, the model can also be applied to particle reinforced composites. In this case, the ratio $\frac{l_f}{d_f}$ is substituted by the aspect ratio of the particle.

## 5.3 Results

A MATLAB program was written and used to evaluate the Halpin-Tsai model for different reinforcement conditions. The script used is shown in Appendix A. The resulting glass fiber composite modulus is plotted against the glass fiber weight fraction in Figure 22. Experimental results and expected material datasheet values are also shown.

The density of kaolin mineral and a range of aspect ratios were provided by the manufacturer. The density was 2.6 g/cm^3 and the aspect ratio was between 70-110. This range of aspect ratios corresponded to the 06XX minerals series. From the properties provided and one experimental data point, a range can be approximated for the modulus of kaolin by backwards solving the Halpin-Tsai equations. Using the modulus of 30% 0641 kaolin composite, the lower bound for the modulus is 68.5 GPa and the upper bound is 72.5 GPa. The Halpin-Tsai equations were then evaluated again for both modulus values (and corresponding aspect ratio) to model the composite modulus vs the weight fraction of 0641 mineral. The result is shown in figure 23. Experimental and literature values are shown as well.
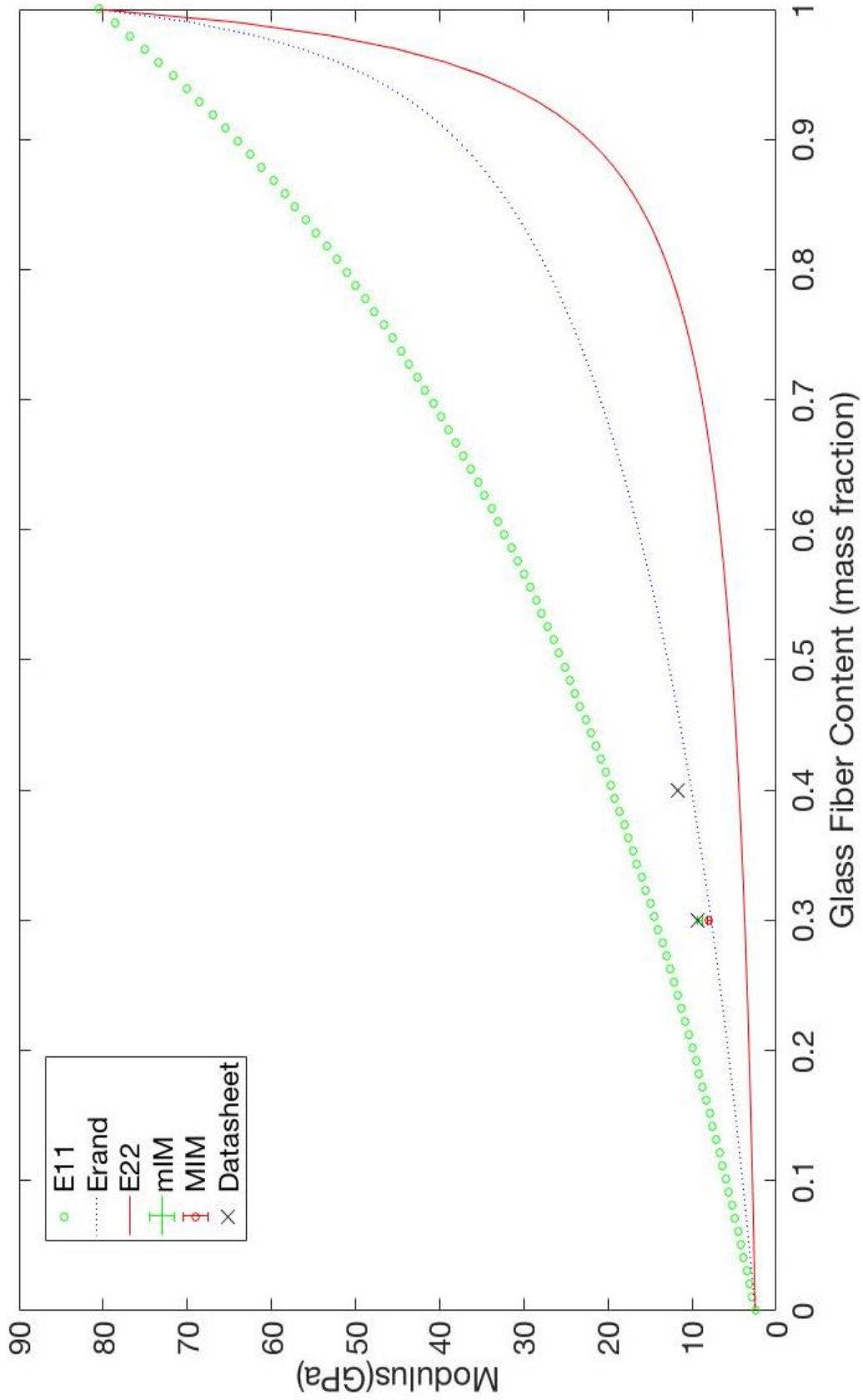
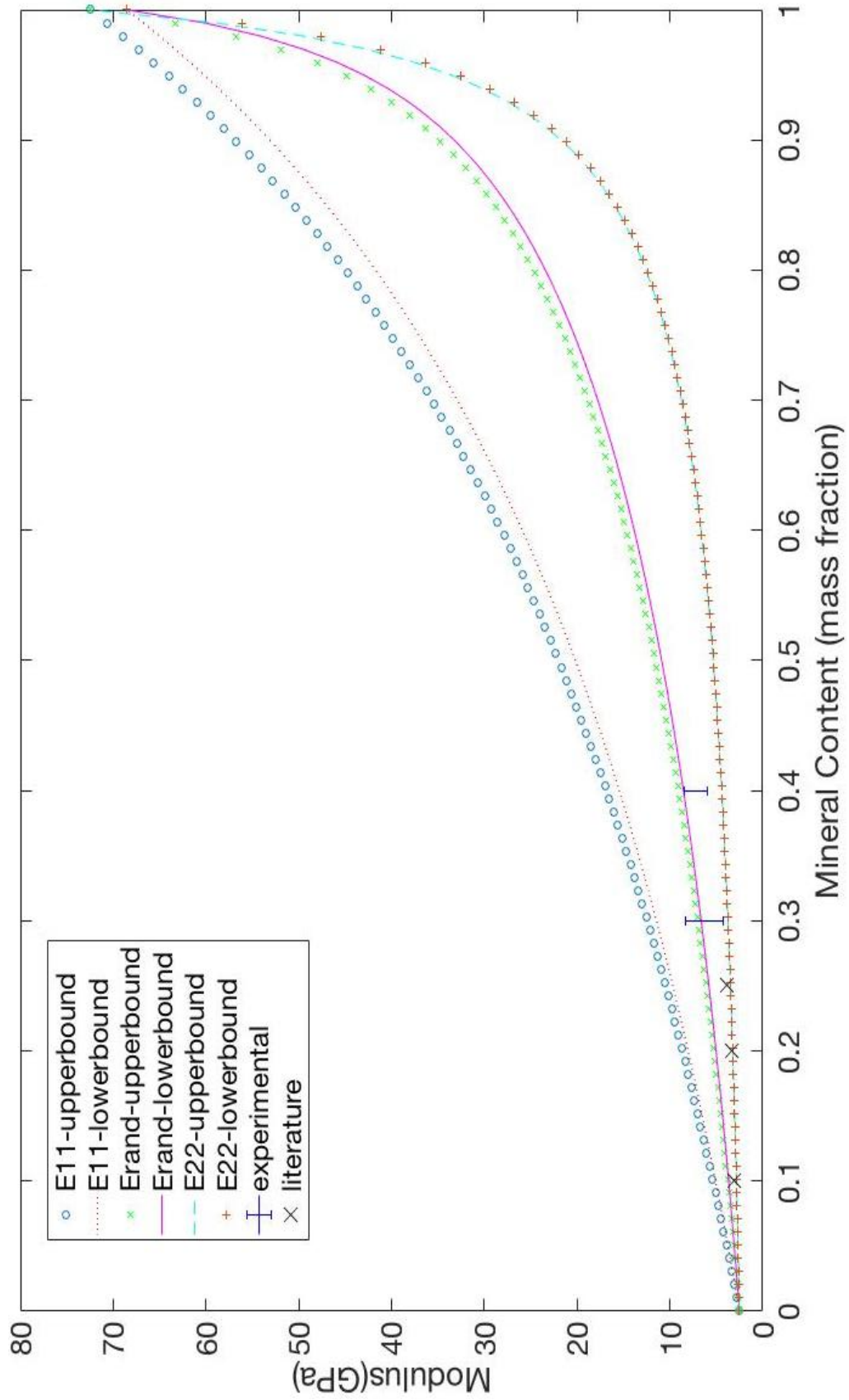**Figure 22 - Modulus vs GF content model and experimental data**

**Figure 23- Modulus of 0641 mineral composites vs mineral content model and experimental**

In Figure 22, $E_{11}$, $E_{22}$, and $E_{rand}$ are represented as seen in the legend. The data point for 30% GF is shown on the graph for both micro scale (mIM) and scale-up fabrication (MIM) methods by green and red error bars respectively. It can be seen that as the fiber content is increased, the predicted random modulus falls closer to $E_{22}$. It is expected that as the fiber content is increased, deviations from longitudinal alignment become more significant driving the modulus closer to the lower bound. The experimental data agrees with the model; however, it is noticed that the model slightly under predicts the modulus. This indicates that the fibers show a degree of preferential alignment in the direction of injection pressure. Another noteworthy observation is that the modulus of the composites made by the lab-scale injection molding unit (mIM)is higher than the modulus of the corresponding composites made by large-scale injection molding (MIM). Processing the material using two step compounding in scale-up fabrication (compounding in tabletop extruder followed by injection molding) could have caused the fiber to break down to shorter strands. This can potentially explain the reduction in modulus despite the higher injection pressure. A comparison between the modulus of the composites made by mIM and the modulus obtained from the material datasheet for glass fiber composites [RTP Co 2017] shows little discrepancy between the two. This indicates that experimental results are in line with expected values.

Figure 23 shows the Halpin-Tsai results for the mineral composites. The upper and lower bound for $E_{11}$, $E_{22}$, and $E_{rand}$ are represented as seen in the legend. Experimental data is shown for 30% and 40% mineral loading. Benchmark data from literature obtained by Unal for non surface treated kaolin at 10, 20, and 25% wt.% loading in a nylon 6 matrix are shown [Unal et al. 2003] [Unal et al. 2004].. The model slightly over predicts the

66

experimental modulus of mineral reinforced samples. The model assumes perfect distribution and no agglomerates, which could explain the over prediction. The results by Unal are expected to be lower due to the absence of surface treatment compared to the kaolin used in this study. However, a similar trend existed showing that increasing kaolin content increased nylon stiffness.

## 5.4    Conclusions

To verify and further understand experimental results, the Halpin-Tsai micromechanical model was used. Experimental results were plotted with model predictions as well as literature and datasheet values. The model under predicts the modulus of glass fiber composites. This can be attributed to preferential alignment of fiber with injection pressure. The tensile modulus of glass fiber composites made using the lab-scale injection molding (mIM) is in agreement with the datasheet values of glass fiber composites whereas the modulus of the corresponding composites made using the scaled-up injection molding (MIM) is slightly lower, which can be explained by the decrease of the fiber length due to extensive compounding. The model over predicts the modulus of mineral composites due to the model's inherent assumption of perfect dispersion. Comparing experimental results to previous studies using untreated kaolin it is found that the treated kaolin exhibits higher modulus values indicating superior reinforcing effects associated with the addition of surface treatement.

The following chapter wraps up the main conclusions obtained from this study. A summary of the experimental approach utilized is presented alongside an overview of obtained results. Recommendations for future work are also highlighted.

# CHAPTER 6.    SUMMARY, RECOMMENEDATIONS, AND FUTURE WORK

An experimental approach was utilized in this study to investigate the possibility of using ultrafine surface treated kaolin mineral fillers as a substitute or a complement to glass fibers in nylon composites. Injection molding at two different scales, lab scale and large-scale, was used to make the composites. A table-top micro extrusion and injection molding unit was used for screening purposes. Mechanical tests indicated that there is a trade off between strength and impact energy depending on the mineral's aspect ratio. Blending of two minerals, one that resulted in composites with high impact strength and one that resulted in composites with high stiffness, produced composites with a very desirable balance between the two properties. Density measurements showed no negative effect on weight associated with substituting glass fibers with mineral composites. Heat distortion temperature testing indicated a strong correlation between HDT and stiffness. In the second phase of the study, composites were made using a 75-ton injection molding machine. Determination of properties showed that the properties of composites made by the scaled-up injection molding machine followed a similar trend to the properties of the composites made using the lab scale technique. This indicates that lab scale fabrication can be used to predict the properties of mineral composites for industrial usage. SEM imaging is used to investigate filler morphology and its distribution within the matrix as well as voids and defects. Failure mechanism included fiber pullouts, fiber breaking, de-bonding between fiber and matrix, and matrix micro cracking. Some deposit features are seen on the surface of glass fibers, potentially indicating an affinity between the mineral and the

fiber. Less agglomeration is seen for specimens with finer particle size fabricated using scale up fabrication. This supports the hypothesis that scale up fabrication improves dispersion. A micromechanical model is employed to compare experimental results to theoretical predictions. The model under predicted the modulus of glass fiber composites compared to experimental results, indicating a degree of alignment. The modulus of mineral filled particles was over predicted suggesting some agglomeration in the experimental batches.

Based on the work done in this thesis, the following recommendations are suggested for future work:

- Further examine the synergistic mechanism between fillers and the associated improvement in properties.

- Develop a parametric model relating mineral combination to composite properties.

- Investigate additional mineral formulations and their corresponding improvement in properties.

- Assess opportunities for further weight reduction through a reduction in mineral content.

- Analyze the associated cost of mineral fillers against glass fibers.

- Explore eliminating the need for a two-step process in scale up manufacturing.

- Study the effects of manufacturing process on filler powder flow as well as fiber breakage.

- Further examine the dimensional stability of mineral composites through studying their coefficient of thermal expansion.

# APPENDIX A. MATLAB SCRIPT USED TO GENERATE HALPIN-

# TSAI MODEL

```matlab
function [E11, E22, Erand] = modulus(wf,lf,tf,pf,Ef)
Em=2.5;
ar=lf./tf;
pm=1.13;
vf=(wf./pf)./((wf./pf)+((1-wf)./pm));
nL=((Ef./Em)-1)./((Ef./Em)+2.*ar);
nT=((Ef./Em)-1)./((Ef./Em)+2);
E11=((1+2.*ar.*nL.*vf).*Em)./(1-nL.*vf);
E22=((1+2.*nT.*vf).*Em)./(1-nT.*vf);
Erand=(3/8).*E11+(5/8).*E22;
end
```

# REFERENCES

Adams, J. M. "Particle Size And Shape Effects In Materials Science: Examples From Polymer And Paper Systems". *Clay Minerals*, vol 28, no. 4, 1993, pp. 509-530. *Mineralogical Society*, doi:10.1180/claymin.1993.028.4.03.

AG, BMW. "BMW I : Concept". *BMW*, 2017, http://www.bmw.com/com/en/insights/corporation/bmwi/concept.html.

Bagherpour, Salar. "Fibre Reinforced Polyester Composites". *Polyester*, 2012, *Intech*, doi:10.5772/48697.

"BASF Ultramid® B27 E 01 PA6 (Dry)". *MatWeb*, 2017, http://www.matweb.com/search/datasheettext.aspx?matguid=4c50851001c54f42aa5a456f10873036.

"Composite Standards". *Astm.Org*, 2017, https://www.astm.org/Standards/composite-standards.html.

Cook, J. et al. "A Mechanism For The Control Of Crack Propagation In All-Brittle Systems". *Proceedings Of The Royal Society A: Mathematical, Physical And Engineering Sciences*, vol 282, no. 1391, 1964, pp. 508-520. *The Royal Society*, doi:10.1098/rspa.1964.0248.

Cox, H L. "The Elasticity And Strength Of Paper And Other Fibrous Materials". *British Journal Of Applied Physics*, vol 3, no. 3, 1952, pp. 72-79. *IOP Publishing*, doi:10.1088/0508-3443/3/3/302.

Das, Sujit. *THE COST OF AUTOMOTIVE POLYMER COMPOSITES: A REVIEW AND ASSESSMENT OF DOE's LIGHTWEIGHT MATERIALS COMPOSITES RESEARCH*. 1st ed., Oak Ridge, TN, Oakridge National Laboratory, 2001, http://www-cta.ornl.gov/cta/Publications/Reports/ORNL_TM_2000_283.pdf.

"Family Of High Modulus (HMG) Nylon Based Plastics Increases Mileage And Reduce Weight". *BASF*, 2001, http://www8.basf.us//PLASTICSWEB/displayanyfile?id=0901a5e180004895.

Fisher, Michael et al. *ENHANCING FUTURE AUTOMOTIVE SAFETY WITH PLASTICS*. 1st ed., https://www-nrd.nhtsa.dot.gov/pdf/esv/esv20/07-0451-w.pdf.

Guessoum, Melia et al. "Effects Of Kaolin Surface Treatments On The Thermomechanical Properties And On The Degradation Of Polypropylene".

*International Journal Of Polymer Science*, vol 2012, 2012, pp. 1-9. *Hindawi Publishing Corporation*, doi:10.1155/2012/549154.

He, Dayong, and Bingzheng Jiang. "The Elastic Modulus Of Filled Polymer Composites". *Journal Of Applied Polymer Science*, vol 49, no. 4, 1993, pp. 617-621. *Wiley-Blackwell*, doi:10.1002/app.1993.070490408.

Iwaya, Tomoko et al. "Kinetic Analysis For Hydrothermal Depolymerization Of Nylon 6". *Polymer Degradation And Stability*, vol 91, no. 9, 2006, pp. 1989-1995. *Elsevier BV*, doi:10.1016/j.polymdegradstab.2006.02.009.

Karian, Harutun G. *Handbook Of Polypropylene And Polypropylene Composites*. 1st ed., Taylor & Francis, 2003,.

Kinloch, A. J. et al. "The Fracture Of Hybrid-Particulate Composites". *Journal Of Materials Science*, vol 20, no. 11, 1985, pp. 4169-4184. *Springer Nature*, doi:10.1007/bf00552413.

Li, Zong-Fu et al. "Fiber Interactions In The Multi-Fiber Composite Fragmentation Test". *Composites Science And Technology*, vol 54, no. 3, 1995, pp. 251-266. *Elsevier BV*, doi:10.1016/0266-3538(95)00056-9.

*Light-Duty Automotive Technology, Carbon Dioxide Emissions, And Fuel Economy Trends: 1975 Through 2016*. 1st ed., 2016, https://www.epa.gov/sites/production/files/2016-11/documents/420r16010.pdf.

MacKenzie, Donald et al. *Determinants Of U.S. Passenger Car Weight*. 1st ed., Cambridge, MA, Massachusetts Institute Of Technology, 2012, http://faculty.washington.edu/dwhm/files/MacKenzie%20Zoepf%20Heywood%20as%20submitted.pdf.

Mallick, P. K. *Fiber-Reinforced Composites*. 1st ed., Boca Raton, Fla. [U.A.], CRC Press, 2008,.

Mareri, P. et al. "Mechanical Behaviour Of Polypropylene Composites Containing Fine Mineral Filler: Effect Of Filler Surface Treatment". *Composites Science And Technology*, vol 58, no. 5, 1998, pp. 747-752. *Elsevier BV*, doi:10.1016/s0266-3538(97)00156-5.

"ME1510 – MULTI END ROVING FOR EPOXY BASED SMC". *Owens Corning*,2014, http://composites.owenscorning.com/uploadedFiles/Composites/Docs/ME1510_product%20sheet_02-2014_Rev0_final(2).pdf.

"Molding Guide: Dupont™ Zytel® HTN High Performance Polyamide". *Dupont*, 2001, http://www.dupont.com/content/dam/dupont/products-and-services/plastics-polymers-and-resins/plastics-polymers-and-resins-landing/documents/H85940.pdf.

"Next-Generation Composites Lighten The Load For Automakers - Automotive Solutions". *BASF,* 2017, http://www.automotive.basf.com/ultracom-lighten-the-load-for-automakers/.

Onuegbu, Genevive C., and Isaac O. Igwe. "The Effects Of Filler Contents And Particle Sizes On The Mechanical And End-Use Properties Of Snail Shell Powder Filled Polypropylene". *Materials Sciences And Applications*, vol 02, no. 07, 2011, pp. 810-816. *Scientific Research Publishing, Inc,*, doi:10.4236/msa.2011.27110.

Raj, Mahendrasinh et al. "Studies On Effects Of Metakaolin As A Filler In Some Commercial Thermoplastics Polymers". *Archives Of Applied Science Research*, vol 7, no. 1, 2015, pp. 1-9.

Riley, A.M. et al. "Factors Affecting The Impact Properties Of Mineral Filled Polypropylene". *Plastics And Rubber Processing And Applications*, vol 14, no. 2, 1990, pp. 85-93.

"RTP 205 A RC HS Black Nylon 6 (PA) Product Data Sheet - RTP Company". *Web RTP Co*, 2017, http://web.rtpcompany.com/info/data/0200A/RTP205ARCHSBlack.htm.

"RTP 207 A RC HS Black Nylon 6 (PA) Product Data Sheet - RTP Company". *Web RTP Co*, 2017, http://web.rtpcompany.com/info/data/0200A/RTP207ARCHSBlack.htm.

Silva, Francisco et al. "Improving The Wear Resistance Of Moulds For The Injection Of Glass Fibre–Reinforced Plastics Using PVD Coatings: A Comparative Study". *Coatings*, vol 7, no. 2, 2017, p. 28. *MDPI AG*, doi:10.3390/coatings7020028.

Švehlová, Vítězslava, and Eduard Polouček. "Journal Search Results - Cite This For Me". *Angewandte Makromolekulare Chemie*, vol 153, no. 1, 1987, pp. 197-200. *Wiley-Blackwell*, doi:10.1002/apmc.1987.051530115.

Tandon, G. P., and G. J. Weng. "The Effect Of Aspect Ratio Of Inclusions On The Elastic Properties Of Unidirectionally Aligned Composites". *Polymer Composites*, vol 5, no. 4, 1984, pp. 327-333. *Wiley-Blackwell*, doi:10.1002/pc.750050413.

Unal, H et al. "Mechanical Properties And Morphology Of Nylon-6 Hybrid Composites". *Polymer International*, vol 53, no. 1, 2004, pp. 56-60. *Wiley-Blackwell*, doi:10.1002/pi.1246.

Unal, H. et al. "Mechanical Behavior Of Nylon Composites Containing Talc And Kaolin". *Journal Of Applied Polymer Science*, vol 88, no. 7, 2003, pp. 1694-1697. *Wiley-Blackwell*, doi:10.1002/app.11927.

Vollenberg, P.H.T. "The Mechanical Behaviour Of Particle Filled Thermoplastics". Technische Universiteit  Eindhoven, Netherlands, 1987,.

Wiebking, Henry. *FILLERS IN PVC A REVIEW OF THE BASICS*. 1st ed., Easton, PA, Minerals Technologies, 1998, http://www.mineralstech.com/Documents/SMI/PM%20-%20Decking/Fillers%20in%20PVC%20-%20A%20Review%20of%20the%20Basics.pdf.

Wolff, Ernest G. *Introduction To The Dimensional Stability Of Composite Materials*. 1st ed., Lancaster, PA, Destech Publ, 2004,.

Zhou, Hongyu et al. "Crashworthiness Characteristics Of A Carbon Fiber Reinforced Dual-Phase Epoxy–Polyurea Hybrid Matrix Composite". *Composites Part B: Engineering*, vol 71, 2015, pp. 17-27. *Elsevier BV*, doi:10.1016/j.compositesb.2014.10.053.